radioimmunoabsorbent assay (RIA; SRL Inc.). The serum level of FGF-2 was monitored by enzyme-linked immunoabsorbent assay (ELISA; Kaken Pharmaceutical Co., Ltd., Tokyo) before and 2, 4, 24, and 2 weeks after the surgery. All patients were also screened for antibodies to FGF-2 and gelatin preoperatively and 2 and 4 weeks postoperatively, by ELISA (Kaken Pharmaceutical Co., Ltd.) and fluorescence enzyme immunoabsorbent assay (FEIA; SRL Inc.), respectively.

Safety Assessment

Safety was monitored according to the number and duration of adverse events. An adverse event was defined as any local or systemic sign, symptom, syndrome, illness, medical condition, or abnormal laboratory data that occurred or worsened after surgery, regardless of causality or treatment group. Infections were conservatively defined as any suspected or confirmed superficial or deep bone or soft-tissue infection, with or without bacteriological confirmation. Retrospectively, all adverse events were classified as serious or nonserious according to ICH Guidelines (International Conference of Harmonization Guideline Clinical Safety Data Management: Definitions and Standards for Expedited Reporting. Federal Register, March 1, 1995).

Statistical Analyses

Baseline characteristics of patients were tested using one-way analysis of varience (ANOVA) or Fisher's exact test. Dose response effects among three dosages of rhFGF-2, and pair-wise comparisons were evaluated by generalized Wilcoxon test and Tukey-Kramer method, respectively. Differences in the number and duration of adverse events were evaluated by Fisher's exact test. Comparison of the serum concentrations was performed with one-way ANOVA and paired t-test. A p-value of <0.05 for analysis of safety variables was considered significant. Data analyses were performed using SAS version 8.0 (SAS Institute Inc., Cary, NC).

RESULTS

Demographics

Fifty-nine patients were enrolled from 16 institutions, and two patients (one for spontaneous retraction of the informed consent and the other for the onset of heart failure) were withdrawn, so that investigations were performed on 57 patients (97%). There were no statistically significant differences (all $p > 0.05$) for any of the baseline data among the groups treated with 200, 400, and 800 μg of rhFGF-2 (Table 1). The low, middle, and high dosage groups consisted of 20, 18, and 19 patients with no significant difference in gender. The average age, body height, weight, and body mass index at surgery were also comparable among the three groups. Although the aimed FTA and the fixation method varied among the institutions, three was no significant difference in the corrected angle or the hardware used among the groups (all $p > 0.05$).

Radiographic Bone Union

The interrater reliability of the three independent reviewers has a weighted kappa coefficient of 0.60–0.68, suggesting an excellent reproducibility among them. All osteotomies were confirmed to show similar bone defects without radiographic

Table 1. Baseline Patient Demographics

	rhFGF-2			
	200 μg	400 μg	800 μg	p-Value
Number of patients	20	18	19	
Males/females	7/13	8/10	11/8	0.378
Age (years) (range)	62.2 ± 9.2 (41–74)	57.4 ± 6.9 (44–72)	59.7 ± 9.7 (40–71)	0.252
Height (cm) (range)	156.7 ± 8.0 (147.0–178.6)	157.1 ± 8.1 (145.8–170.0)	159.3 ± 9.4 (142.3–175.0)	0.603
Weight (kg) (range)	63.9 ± 9.6 (50.0–84.0)	68.1 ± 10.7 (51.0–88.3)	64.8 ± 9.8 (43.0–82.5)	0.415
Body mass index (kg/m^2) (range)	26.0 ± 3.2 (21.3–34.5)	27.6 ± 4.5 (22.4–36.9)	25.5 ± 2.7 (19.1–28.5)	0.167
Corrected angle (degrees)				0.847
<10	0	1	1	
10–14	10	9	7	
15–19	8	5	9	
≥20	2	3	2	
Fixation methods				0.177
External fixation	12	5	7	
Internal plate fixation	6	12	11	
Internal stabple fixation	2	1	1	

Data are mean ± SD.

DOI 10.1002/jor

bone union at time 0. The rhFGF-2 dose dependently increased the percentage of patients with radiographic bone union during the observation period up to 16 weeks ($p = 0.015$ between the high and low dosage groups; $p = 0.035$ among the three groups) (Fig. 1A). The percentages of patients with radiographic bone union in the high dosage group was about three times and twice those in the low dosage group at 8 and 10 weeks, respectively. At 12 weeks and thereafter, even the low dosage group showed radiographic bone union, and eventually at 16 weeks all patients achieved radiographic bone union. All patients with bone union at earlier time points were confirmed to conserve the status until the last visit at 16 weeks without refracture. The times needed for 50% of patients in the low, middle, and high dosage groups to show radiographic bone union were 11.5, 10.1, and 8.1 weeks, respectively (Fig. 1A). In the meantime, the average times needed for radiographic bone union in the three groups were 11.5, 9.3, and 9.0 weeks, respectively (Fig. 1B). Figure 2 shows the time course of X-ray pictures of representative patients in the three groups. In the patients of the low dosage group, the bony bridging across the osteotomy gap was not apparent even at 10 weeks. In patients of middle and high dosage groups, on the contrary, the calcified callus was observed at 6 weeks and the bony bridging at 8 weeks following the surgery.

Clinical Outcomes

We next examined the effects of rhFGF-2 on clinical outcomes. The percentages of patients who were pain free at the osteotomy site, those with full-weight bearing on the operated leg, and those with clinical healing (defined as both radiographic bone union and pain free) were higher in middle- and high-dosage groups than in the low-dosage group, especially in the clinically critical periods 6, 8, and 10 weeks after the surgery (Fig. 3). However, at 12 weeks and thereafter, even the low-dosage group showed comparable clinical outcomes to the higher groups, just like radiographic bone union. All patients deemed clinically healed at earlier time points were confirmed to have conserved that status until the last visit without recurring pain or fracture.

Blood Chemistries

The serum calcium, phosphate, calcitonin, and osteocalcin levels were measured preoperatively, and 2 and 4 weeks postoperatively. No significant

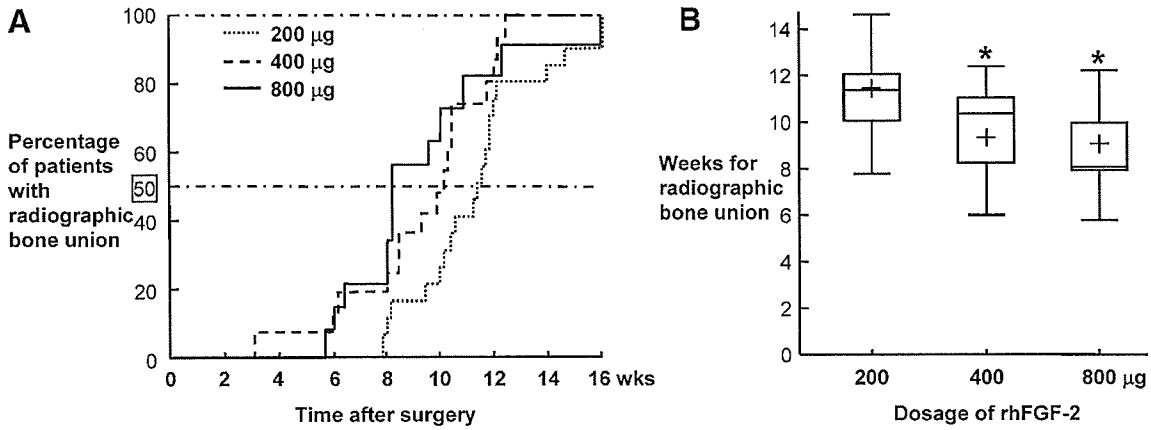

Figure 1. Comparison of radiographic bone union among patients with 200, 400, and 800 μg rhFGF-2 application. Radiographic bone union was defined as the apparent bridging by bony beam across the osteotomy gap on standard X-ray pictures that were taken immediately after the surgery and at least every 2 weeks threafter up to 16 weeks. (A) Time course of the percentage of patients with radiographic bone union during 16 weeks after the surgery in the three dosage groups. rhFGF-2 dose dependently increased the percentage of those with radiographic bone union ($p = 0.035$ among the three groups, and $p = 0.015$ between the high and low dosage groups). (B) Box and whisker plot representing weeks needed for radiographic bone union in the three dosage groups. The line through the box is the median; the top and bottom edges of each box represent the 25 and 75 percentiles, giving the interquartile range; and cross in the box is the mean. The vertical lines at each side of the box represent distribution from the quartiles to the farthest observation. $^*p < 0.05$; significant difference from the 200 μg group by the Tukey-Kramer test.

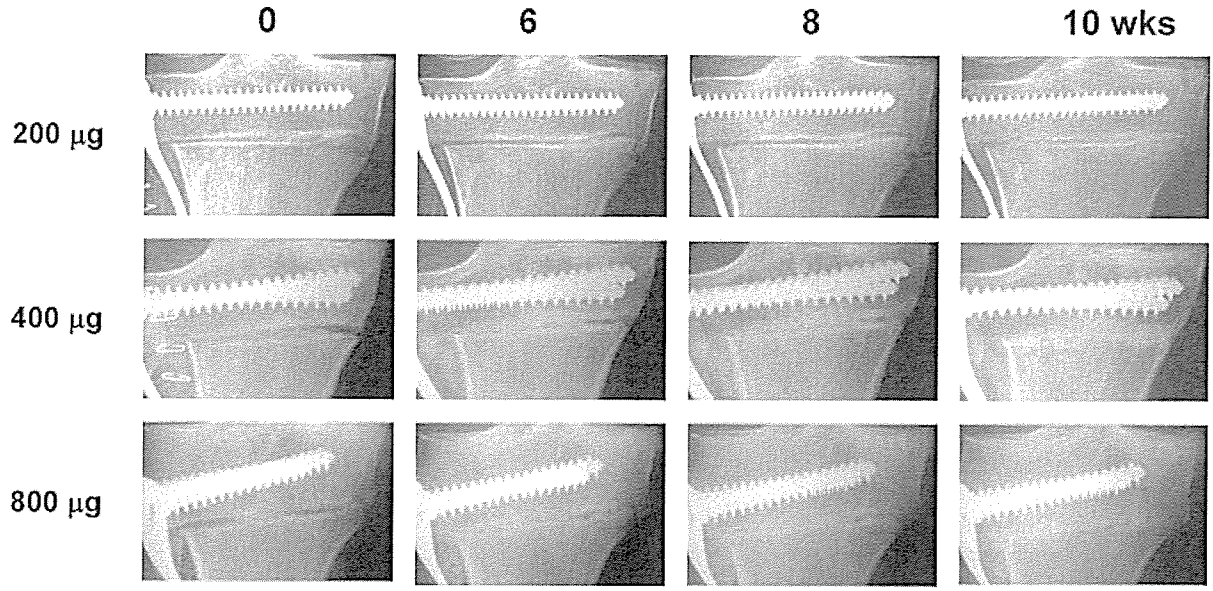

Figure 2. Anteroposterior X-ray pictures of tibial osteotomy sites of representative patients in the three dosage groups at 0, 6, 8, and 10 weeks after the surgery.

difference was detected in the calcium, phosphate, or osteocalcin levels among the three dosage groups, nor among the time points before and after the surgery (all $p > 0.05$). Although only the preoperative calcitonin level was higher in the low- dosage group, the levels became comparable after the surgery. The serum FGF-2 level also was not significantly affected by the dosage of applied rhFGF-2 at least up to 2 weeks after the application (all $p > 0.05$). Neither antibody to FGF-2 nor that to gelatin was detected in any patients preoperatively or postoperatively.

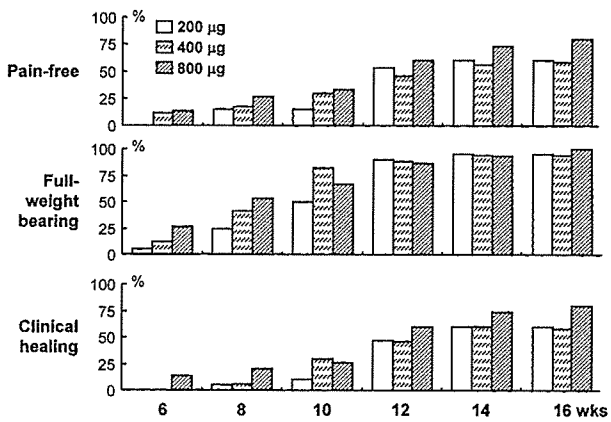

Figure 3. Comparison of clinical outcomes among patients with 200, 400, and 800 μg rhFGF-2 application. Cumulative percentage of patients with absence of pain at the osteotomy site, those with full weight bearing on the operated leg, and those with clinical healing (defined as both radiographic bone union and absence of pain) were compared every 2 weeks for 16 weeks after the surgery. The missing data of only one patient in the 400 μg group at 6 weeks were carried forward from those at 4 weeks.

Safety

The local or systemic adverse events experienced by the patients during the observation periods included several kinds of skin disorders, peroneal palsy, coryza, fever, and diarrhea (Table 2). Of the local skin disorders, the pin-site infection was most frequent and lasted 7–49 days. The durations of other systemic or local skin disorders such as eczema, eruption, and edema ranged 1–52 days. Two cases of peroneal palsy that were seen in the operated leg of the low dosage group lasted 28 and 105 days after surgery, and recovered within the obsevation period. Other systemic disorders: coryza, fever, and diarrhea were also temporary, and lasted 1–33 days. All the symptoms were classified as nonserious according to ICH Guidelines. Although the knee range of motion was not evaluated, there was no report of the disability as an adverse event. There was no case with hardware failure of the fixation device nor with heterotopic ossification of ligaments, tendons, or cartilage on X-ray during the obsevation periods. Regarding laboratory data, increases in the serum levels of C-reactive protein and fibrinogen levels may be due to the pin-infection, because both decreased to normal levels with disappearance of the infection. Slight increases in the glutamate–pyruvate–transaminase and eosinophil levels

DOI 10.1002/jor

Table 2. Adverse Events

	rhFGF-2			
	200 μg	400 μg	800 μg	Total
Local events				
Skin disorders				
Pin site infection	4	2	1	7
Eczema	0	0	1	1
Peroneal palsy	2	0	0	2
Systemic events				
Skin disorders				
Eczema	2	3	3	8
Eruption	1	1	2	4
Edema	0	0	3	3
Coryza	3	3	4	10
Fever	0	1	2	3
Diarrhea	0	0	1	1
Laboratory data				
C-reactive protein increase	2	0	1	3
Fibrinogen increase	0	0	1	1
Glutamate-pyruvate-transaminase increase	1	0	0	1
Eosinophil increase	1	0	0	1

were detected within 4 weeks after the surgery, and decreased to normal levels thereafter. All of these symptoms and abnormal laboratory data had recovered before the last visit at 16 weeks, and neither the number nor the duration statistically showed positive association with the dosages of the rhFGF-2 applied.

DISCUSSION

Based on the evidence of extensive studies using various animal models,[6–15] this study for the first time showed clinical evidence that rhFGF-2 in gelatin hydrogel accelerated radiographic bone union of the closing wedge high tibial osteotomy. Because most osteotomies can heal only with appropriate fixations, and in fact, all patients even of the low dosage group eventually achieved radiographic bone union in the present study, the rhFGF-2 application may not have yielded bone union by preventing nonunion, but just accelerated bone union. However, if the osteotomy site remains unstable for a long time, the chances of mal-union and infection causing skeletal deformity, late nerve palsy and refracture may increase. The reduction of time for bone union by the rhFGF-2 application is therefore important not only for the comfort of the patient after surgery, but also for the prevention of these secondary disorders.

FGF-2 is reported to stimulate the proliferation of immature mesenchymal cells but to inhibit the differentiation and matrix synthesis of osteoblastic cells.[18–22] Our preliminary experiments using the rat and rabbit models demonstrated that the local half-life of the injected ^{125}I-labeled FGF-2 in the gelatin hydrogel was 1 to 2 days. The percentages of the ^{125}I-labeled FGF-2 remaining localized were approximately 20, 3, and 1% at 1, 2, and 3 weeks, respectively. Hence, FGF-2 appears to have its effect primarily in the earlier stage of bone repair, probably through its mitogenic action on immature mesenchymal cells. In fact, previous animal studies demonstrated that a single injection of FGF-2 enhanced the proliferation of chondroprogenitor cells in fracture callus, causing the formation of a larger cartilage, but did not directly affect maturation of chondrocytes or replacement of the cartilage by osseous tissue.[7,14,23] Furthermore, expressions of FGF-2, FGF-1, and their principal receptor FGFR1 have been identified mainly at the early stage of fracture healing.[1,24–26] In addition to its mitogenic action on immature mesenchymal cells, FGF-2 may induce other anabolic factors such as prostaglandins, transforming growth factor (TGF)-β and bone morphogenetic proteins (BMPs), which may compose a serial cascade of bone formation. In fact, we and others have shown that FGF-2 induces TGF-β expression and prostaglandin production in a rat fracture model and in cultured osteoblastic cells.[7,27,28] Because the present blood chemistries indicate the absence of influence on systemic bone turnover and metabolism, FGF-2 may act as a local

factor that initiates the cascade of bone formation in the entire bone repair process. The follow-up period for 16 weeks might be relatively short for the safety conclusions. However, considering the above pharmacokinetics of rhFGF-2 in the gelatin hydrogel, we assume that the effect may possibly not persist after 16 weeks.

Among growth factors that have been investigated to date, BMPs appear to be the most popular that exhibit a potent osteoanabolic activity. Unlike FGF-2, BMPs strongly stimulate the differentiation and matrix synthesis of osteoprogenitor cells.[29,30] Regarding the clinical applications, three randomized trials have led to various regulatory agency approvals for specific indications of rhBMPs in the United States and other countries.[31–33] Two of them showed the positive effects on bone repair: one for rhBMP-2 on open tibial fractures[32] and the other for rhBMP-7 (rhOP-1) on tibial nonunions.[33] However, considering that as much as 12 mg of rhBMP-2 and 3.5 mg of rhBMP-7 were needed to show positive effects in those studies, bone anabolic potencies of the BMPs in clinical settings are not as impressive as those seen in animal models in which more robust bone formation and healing have been observed.[29,30] This may be because BMPs may be degraded more quickly in humans than in animals, the biology of the receptor–ligand interactions may differ, or the pharmacokinetics of the activity may be less favorable in humans.

The most important limitation of the present study is the lack of the vehicle control group (the gelatin hydrogel only). IRB of several institutions did not deem it ethically acceptable because systemic immediate-type reactions, including anaphylactic shock, to measles, mumps, rubella, and varicella vaccines reported in some children were suspected to be allergic symptoms caused by gelatin antigen that is included in the vaccines as a stabilizer.[34] The present gelatin hydrogel was therefore originally synthesized by deleting the antigenic portion.[16,17] We believe that the present result showing the absence of the antibody in the patients may lead to the approval of the clinical use of the gelatin hydrogel as the rhFGF-2 carrier. Instead of the control group, we determined the three dosages of rhFGF-2 based on previous preclinical results of osteotomy experiments on animals.[7–9,12] When the dosages in the animal studies were converted to the area of the human proximal tibiae, 800 μg of rhFGF-2 was expected to show a significant anabolic function, while 200 μg exerted little effect. In fact, the high dosage of rhFGF-2 showed significant bone anabolic function over the low dosage in the present clinical study. Furthermore, all patients of the low-dosage group also eventually achieved bone union after 16 weeks, although a previous report on the natural course of high tibial osteotomy showed that 8.5 and 5.7% remained nonunion even after 6 months and 1 year, respectively.[35] Hence, unlike BMPs, the discrepancy of bone anabolic potency between animals and humans may not be seen in the function of FGF-2. However, because the rationale for the present dose selection was not based on prior clinical evaluations to determine the dose with maximum efficacy, we are now planning a clinical trial using higher amounts of rhFGF-2.

In conclusion, the present dose–escalation clinical trial revealed that rhFGF-2 in gelatin hydrogel dose dependently accelerated bone repair of the tibial osteotomy with a safety profile. Because the formulation of the rhFGF-2 gelatin hydrogel is slightly viscid, it not only can be applied to the osteotomy site during the surgical procedure, but also can be percutaneously injected under roentgenologic guidance at the time of closed reduction of a bone fracture followed by a fixation with casting. We are now planning a more advanced clinical trial on fresh tibial fractures including a control group for the application of regulatory agency approval to obtain clinical indication of this agent. Furthermore, the development of appropriate delivery systems may yield progress; for example, a sequential delivering system of FGF-2 at the earlier stage and other differentiation factors like BMPs at the later stage might have potential as the optimal method of inducing bone formation. The extensive application of the osteoanabolic nature of FGF-2 to various skeletal disorders will be explored in the near future.

ACKNOWLEDGMENTS

This work was supported by Grants-in-Aid for Scientific Research from the Japanese Ministry of Education, Culture, Sports, Science and Technology, which had no role in study design, data collection, data analysis, data interpretation, or writing of the report. We declare that we have no conflict of interest.

REFERENCES

1. Lieberman JR, Daluiski A, Einhorn TA. 2002. The role of growth factors in the repair of bone biology and clinical applications. J Bone Joint Surg [Am] 84:1032–1044.
2. Itoh N, Ornitz DM. 2004. Evolution of the Fgf and Fgfr gene families. Trends Genet 20:563–569.
3. Canalis E, Centrella M, McCarthy T. 1988. Effects of basic fibroblast growth factor on bone formation in vitro. J Clin Invest 81:1572–1577.

4. Khan SN, Bostrom MP, Lane JM. 2000. Bone growth factors. Orthop Clin North Am 31:375–388.
5. Coumoul X, Deng CX. 2003. Roles of FGF receptors in mammalian development and congenital diseases. Birth Defects Res C Embryo Today 69:286–304.
6. Aspenberg P, Lohmander LS. 1989. Fibroblast growth factor stimulates bone formation. Acta Orthop Scand 60: 473–476.
7. Kawaguchi H, Kurokawa T, Hanada K, et al. 1994. Stimulation of fracture repair by recombinant human basic fibroblast growth factor in normal and streptozotocin-diabetic rats. Endocrinology 135:774–781.
8. Kato T, Kawaguchi H, Hanada K, et al. 1998. Single local injection of recombinant fibroblast growth factor-2 stimulates healing of segmental bone defects in rabbits. J Orthop Res 16:654–659.
9. Nakamura T, Hara Y, Tagawa M, et al. 1998. Recombinant human basic fibroblast growth factor accelerates fracture healing by enhancing callus remodeling in experimental dog tibial fracture. J Bone Miner Res 13:942–949.
10. Radomsky ML, Aufdemorte TB, Swain LD, et al. 1999. Novel formulation of fibroblast growth factor-2 in a hyaluronan gel accelerates fracture healing in nonhuman primates. J Orthop Res 17:607–614.
11. Tabata Y, Yamada K, Hong L, et al. 1999. Skull bone regeneration in primates in response to basic fibroblast growth factor. J Neurosurg 91:851–856.
12. Kawaguchi H, Nakamura K, Tabata Y, et al. 2001. Acceleration of fracture healing in non-human primates by fibroblast growth factor-2. J Clin Endocrinol Metab 86:875–880.
13. Okazaki H, Kurokawa T, Nakamura K, et al. 1999. Stimulation of bone formation by recombinant fibroblast growth factor-2 in callotasis bone lengthening of rabbits. Calcif Tissue Int 64:542–546.
14. Nakamura K, Kawaguchi H, Aoyama I, et al. 1997. Stimulation of bone formation by intraosseous application of recombinant basic fibroblast growth factor in normal and ovariectomized rabbits. J Orthop Res 15:307–313.
15. Nakamura T, Hanada K, Tamura M, et al. 1995. Stimulation of endosteal bone formation by systemic injections of recombinant basic fibroblast growth factor in rats. Endocrinology 136:1276–1284.
16. Tabata Y, Ikada Y. 1999. Vascularization effect of basic fibroblast growth factor released from gelatin hydrogels with different biodegradabilities. Biomaterials 20:2169–2175.
17. Tabata Y, Nagano A, Ikada Y. 1999. Biodegradation of hydrogel carrier incorporating fibroblast growth factor. Tissue Eng 5:127–138.
18. Hurley MM, Abreu C, Harrison JR, et al. 1993. Basic fibroblast growth factor inhibits type I collagen gene expression in osteoblastic MC3T3-E1 cells. J Biol Chem 268:5588–5593.
19. Hurley MM, Kessler M, Gronowicz G, et al. 1992. The interaction of heparin and basic fibroblast growth factor on collagen synthesis in 21-day fetal rat calvariae. Endocrinology 130:2675–2682.
20. Kato Y, Iwamoto M. 1990. Fibroblast growth factor is an inhibitor of chondrocyte terminal differentiation. J Biol Chem 265:5903–5909.
21. McCarthy TL, Centrella M, Canalis E. 1989. Effects of fibroblast growth factors on deoxyribonucleic acid and collagen synthesis in rat parietal bone cells. Endocrinology 125:2118–2126.
22. Rodan SB, Wesolowski G, Kyonggeun Y, Rodan GA. 1989. Opposing effects of fibroblast growth factor and pertussis toxin on alkaline phosphatase, osteopontin, osteocalcin and type I collagen mRNA levels in ROS 17/2.8 cells. J Biol Chem 264:19934–19941.
23. Nakajima F, Ogasawara A, Goto K, et al. 2001. Spatial and temporal gene expression in chondrogenesis during fracture healing and the effects of basic fibroblast growth factor. J Orthop Res 19:935–944.
24. Bolander ME. 1992. Regulation of fracture repair by growth factors. Proc Soc Exp Biol Med 200:165–170.
25. Bourque WT, Gross M, Hall BK. 1993. Expression of four growth factors during fracture repair. Int J Dev Biol 37: 573–579.
26. Nakajima A, Nakajima F, Shimizu S, et al. 2001. Spatial and temporal gene expression for fibroblast growth factor type I receptor (FGFR1) during fracture healing in the rat. Bone 29:458–466.
27. Kawaguchi H, Pilbeam CC, Gronowicz G, et al. 1995. Transcriptional induction of prostaglandin G/H synthase-2 by basic fibroblast growth factor. J Clin Invest 96:923–930.
28. Noda M, Vogel R. 1989. Fibroblast growth factor enhances type β1 transforming growth factor gene expression in osteoblast-like cells. J Cell Biol 109:2529–2535.
29. Einhorn TA. 2003. Clinical applications of recombinant human BMPs: early experience and future development. J Bone Joint Surg [Am] 85:82–88.
30. Luppen CA, Blake CA, Ammirati KM, et al. 2002. Recombinant human bone morphogenetic protein-2 enhances osteotomy healing in glucocorticoid-treated rabbits. J Bone Miner Res 17:301–310.
31. Burkus JK, Gornet MF, Dickman CA, et al. 2002. Anterior lumbar interbody fusion using rhBMP-2 with tapered interbody cages. J Spinal Disord Tech 15:337–349.
32. Govender S, Csimma C, Genant HK, et al. 2002. Recombinant human bone morphogenetic protein-2 for treatment of open tibial fractures: a prospective, controlled, randomized study of four hundred and fifty patients. J Bone Joint Surg [Am] 84:2123–2134.
33. Friedlaender GE, Perry CR, Cole JD, et al. 2001. Osteogenic protein-1 (bone morphogenetic protein-7) in the treatment of tibial nonunions. J Bone Joint Surg [Am] 83(Suppl):151–158.
34. Sakaguchi M, Inouye S. 2000. Systemic allergic reactions to gelatin included in vaccines as a stabilizer. Jpn J Infect Dis 53:189–195.
35. Naudie D, Bourne RB, Rorabeck CH, et al. 1999. Survivorship of the high tibial valgus osteotomy. A 10- to -22-year followup study. Clin Orthop Relat Res 367: 18–27.

The FASEB Journal Express article fj.06-7571com. Published online February 22, 2007.

The FASEB Journal • Research Communication

Identification of a potent combination of osteogenic genes for bone regeneration using embryonic stem (ES) cell-based sensor

Shinsuke Ohba,[*,†,‡] Toshiyuki Ikeda,[†] Fumitaka Kugimiya,[†,‡] Fumiko Yano,[†,‡] Alexander C. Lichtler,[§] Kozo Nakamura,[†] Tsuyoshi Takato,[†] Hiroshi Kawaguchi,[†] and Ung-il Chung[‡,1]

[*]Japan Society for the Promotion of Science (JSPS), Chiyoda-ku, Tokyo, Japan; [†]Division of Sensory and Motor System Medicine and [‡]Center for Disease Biology and Integrative Medicine, Faculty of Medicine, the University of Tokyo, Hongo, Bunkyo-ku, Tokyo, Japan; and [§]Department of Genetics and Developmental Biology, University of Connecticut Health Center, Farmington, Connecticut, USA

ABSTRACT **To identify potent bioactive factors for *in vivo* tissue regeneration by comprehensive screening remains a challenge for regenerative medicine. Here we report the development of an ES cell-based monitoring system for osteogenic differentiation, the identification of a potent combination of osteogenic genes using such a system, and an evaluation of its therapeutic potentials. ES cells were isolated from mice carrying a transgene expressing GFP driven by the 2.3 kb fragment of rat type I collagen α(1) promoter. Using these cells engineered to fluoresce on osteogenic differentiation, we screened cDNA libraries and combinations of major osteogenesis-related genes. Among them, the combination of constitutively active activin receptor-like kinase 6 (caALK6) and runt-related transcription factor 2 (Runx2) was the minimal unit that induced fluorescence. The combination efficiently induced osteogenic differentiation in various cell types, including terminally differentiated nonosteogenic cells. The cooperative action of the combination occurred through protein stabilization of core binding factor beta (Cbfb), induction of Runx2-Cbfb complex formation, and its DNA binding. Furthermore, transplantation of a monolayer sheet of fibroblasts transduced with the combination achieved bone regeneration within 4 wk in mouse calvarial bone defects. Thus, we successfully identified the potent combination of genes for bone regeneration, which helped broaden cell sources.—Ohba, S., Ikeda, T., Kugimiya, F., Yano, F., Lichtler, A. C., Nakamura, K., Takato, T., Kawaguchi, H., Chung, U. I. Identification of a potent combination of osteogenic genes for bone regeneration using embryonic stem (ES) cell-based sensor. *FASEB J.* 21, 000–000 (2007)**

Key Words: osteogenesis · screening · biosensor · cell sheet

TRAUMA, DISEASE, AND DEVELOPMENTAL abnormalities resulting in skeletal defects often incur considerable morbidity (1). Bone grafts and prosthetic implant devices are the current strategies to repair irreversible skeletal damages. However, the bone grafts have shortcomings concerning both quantity (availability of bone graft material) and quality (donor site troubles, graft rejection, and disease transmission), and the prosthetic implants have shortcomings concerning quality (biocompatibility, function, and longevity). Regenerative medicine using the technique of tissue engineering attempts to provide solutions to such problems (2).

There are three components important for tissue regeneration: scaffolds, cells, and signaling pathways. Among them, autologous cell transplantation of mesenchymal stromal cells (MSCs) derived from bone marrow and adipose tissue using biodegradable scaffolds have been widely used in bone regeneration (3–6). However, MSCs are limited both in quantity and differentiation capacity. Their definition is vague; it is controversial whether they are real stem cells that require the ability for self-renewal and multipotency. From 10 ml of bone marrow fluid or adipose tissue, only 10^3 to 10^6 cells can be isolated (3, 7). To regenerate clinical bone defects, ~10^9 cells may be required (3), but it is difficult to expand MSCs by several rounds of passages without affecting their differentiation capacity (8). On the other hand, ES cells and multipotent adult progenitor cells are virtually unlimited in quantity; however, it is difficult and costly to isolate these cells, and their differentiation efficiency seems restricted (9–11). In short, the use of stem cells has not yet overcome these crucial hurdles and a new strategy needs to be developed. One solution for this conundrum is to establish a method to control osteoblast differentiation independent of cell sources and to apply this method to abundant autologous adult cells such as dermal fibroblasts for *in vivo* bone regeneration. For this purpose, we need to identify potent

[1] Correspondence: Center for Disease Biology and Integrative Medicine, Faculty of Medicine, the University of Tokyo, 7–3-1 Hongo, Bunkyo-ku, Tokyo 113-0033, Japan. E-mail: uichung-tky@umin.ac.jp

doi: 10.1096/fj.06-7571com

signals that can induce osteogenic differentiation even in nonosteogenic, nonstem cells.

Substantial progress has been made in the basic understanding of major osteogenic signaling molecules and genes such as bone morphogenetic proteins (BMPs), Hedgehogs, Runx2, Wnts, and insulin-like growth factors (IGFs) (12–16). Each factor, however, was effective on specific cell types, including stem cells and osteoblast progenitors (12, 17). In addition, although most of these individual molecules are endogenously expressed in various tissues, the region where osteogenesis occurs is restricted. These data suggest that these individual factors are not potent enough and that ideal signaling may be achieved by a new factor or combinations of factors.

In this study, we developed an ES cell-based monitoring system for osteogenic differentiation that enabled us to identify a potent combination of osteogenic genes through a convenient, reliable screening method. We then investigated the molecular mechanisms underlying the cooperative action of components of the combination. Finally, we tested its *in vivo* relevance through transplantation of skin fibroblasts transduced with it into the mouse bone defect model.

MATERIALS AND METHODS

Construction of retroviral cDNA library and functional cloning

Mouse cDNA libraries were constructed with mRNA isolated from mouse embryos at embryonic day 13.5 or 15.5. cDNAs were cloned unidirectionally into the pMX-Puro vectors. These vectors were transfected to platinum E cells using Fugene6 (Roche, Penzberg, Germany) according to the manufacturer's instructions and the cells were cultured for 48 h. The retroviral supernatant was infected into Col1a1GFP ES cells and cultured for 10 days. GFP fluorescence was observed using a fluorescence microscope.

Preparation of adenoviruses and plasmids

Adenoviral expression vectors encoding rat caSmoothened (caSmo) (18), *myc*-tagged human GLI3C'Δ*Cla*I (19), hemagglutinin (HA) -tagged mouse ca lymphoid enhancer factor 1 (LEF-1), HA-tagged mouse dominant negative (dn) LEF-1 (20), and mouse core binding factor beta (Cbfb; a generous gift from T. Komori, Nagasaki University, Nagasaki, Japan) were constructed using the AdenoX Expression System (Clontech, Palo Alto, CA, USA), according to the manufacturer's instructions. Adenoviruses expressing mouse Runx2 and Flag-tagged mouse dnRunx2 were generous gifts from R. Nishimura (Osaka University, Osaka, Japan); adenoviruses expressing HA-tagged mouse caALK6 and Flag-tagged mouse Smad6 from K. Miyazono (the University of Tokyo, Tokyo, Japan); adenoviruses expressing HA-tagged human insulin receptor substrate 1 (IRS-1) and HA-tagged human dnIRS-1 from W. Ogawa (Kobe University, Kobe, Japan).

Cell culture

NIH3T3 and HeLa were obtained from the Riken Cell Bank (Tsukuba, Japan) and the JCRB Cell Bank (Osaka, Japan), respectively; mesenchymal stromal cells (hMSCs) and human dermal fibroblasts (hDFs) were from Cambrex (East Rutherford, NJ, USA). Wild-type (WT) calvaria cells were isolated from C57BL/6N mice as described (16). Cbfb−/− calvaria cells were generous gifts from T. Fujita and T. Komori (Nagasaki University, Nagasaki, Japan). These cells were maintained in high glucose Dulbecco's modified Eagle medium (DMEM) (Sigma-Aldrich, St. Louis, MO, USA) containing 10% FBS (Sigma-Aldrich), 50 U/ml penicillin, and 50 μg/ml streptomycin (Sigma-Aldrich). Col1a1GFP-ES cells were isolated as described (21) from blastocysts carrying the Col1a1GFP transgene obtained by mating Col1a1GFP transgenic mice with WT mice. Maintenance of isolated ES cells, formation of embryoid bodies (EBs), and induction of their subsequent differentiation were performed as described (9, 22).

For functional cloning using retroviral cDNA libraries, the retroviral supernatant was used to infect Col1a1GFP ES cells and was cultured for 10 days. For screening of adenoviral vectors, each adenovirus was infected at 50 multiplicities of infection. After infection, the cells were cultured in DMEM supplemented with 1× insulin-transferin-selenium + 1 (Sigma-Aldrich) and 1% penicillin/streptomycin (serum-free DMEM) or serum-free osteogenic medium, which is serum-free DMEM supplemented with 0.1 μM dexamethasone (Sigma-Aldrich), 50 mM β-glycerophosphate (Sigma-Aldrich), and 50 μg/ml ascorbic acid phosphate (Wako Pure Chemicals Industry, Ltd., Osaka, Japan). For an analysis of calcification, von Kossa staining was performed as described (23).

Real-time RT-polymerase chain reaction (real-time RT-PCR)

Total RNA was extracted using an ISOGEN Kit (Wako Pure Chemicals Industry, Ltd., Tokyo, Japan) and treated with DNase I (Qiagen, Hilden, Germany). After reverse transcription using a Takara RNA PCR Kit, AMV version 2.1 (Takara Shuzo Co., Shiga, Japan), PCR was performed with the ABI Prism 7000 Sequence Detection System (Applied Biosystems, Foster City, CA, USA) and QuantiTect SYBR Green PCR Master Mix (Qiagen), according to the manufacturer's instructions. The mRNA copy number of a specific gene in the total RNA was calculated as described (23). All reactions were run in triplicate. The primer sequences are available upon request.

Immunoblot and coimmunoprecipitation

Preparation of whole cell lysates was performed using a radio-immunoprecipitation assay buffer as described (24). Separated extraction of cytoplasmic and nuclear proteins was performed using an NE-PER Kit (Pierce Chemical Co., Rockford, IL, USA). Immunoblotting was performed as described (22) using anti-HA mouse monoclonal antibody (mAb) (1:1000; Santa Cruz Biolaboratories, Santa Cruz, CA, USA), anti-Flag rabbit antibody (1:1000; Sigma-Aldrich), anti-Myc antibody (1:1000; Upstate, Lake Placid, NY, USA), anti-Smo rabbit polyclonal antibody (pAb) (H-300, 1:200; Santa Cruz Biolaboratories), anti-Runx2 mouse mAb (1:1000; MBL, Nagoya, Japan), anti-PEBP2β mouse mAb (1:1000; MBL), or anti-actin rabbit antibody (1:1000; Sigma-Aldrich). Secondary antibodies (HRP-conjugated goat anti-mouse IgG or goat anti-rabbit IgG; Promega, Madison, WI, USA) were used at a dilution of 1:10,000.

Coimmunoprecipitation assays were performed using a Catch and Release kit (Upstate) according to the manufacturer's instructions. After being treated with 100 μg of dithiobis (succinimidyl propionate, a reducible chemical cross-linker) (DSP, Pierce Chemical Co.) per milliliter for 20

min, the cell lysates were incubated with 5 μg of anti-Runx2 antibodies at 4°C for 4 h. Immune complexes were eluted and subjected to SDS-PAGE.

Chromatin immunoprecipitation (ChIP)

ChIP was performed using a Chromatin Immunoprecipitation (ChIP) Assay Kit (Upstate), 5 μg of anti-Runx2 antibodies, and 5 μg of anti-PEBP2β antibodies according to the manufacturer's instructions. PCR was performed to amplify the promoter region of the osteocalcin gene containing OSE2 site. The primer sequences are available upon request.

Generation of mouse dermal fibroblast (mDF) cell sheets

Skin tissues were obtained from the backs of 8-wk-old male transgenic mice expressing GFP ubiquitously (C57BL/6-Tg-N(act-enhanced GFP (EGFP))OsbC14-Y01-FM131, GFP transgenic mice, Riken Bioresource Center, Tsukuba, Japan). Isolation of mDFs was performed as described (25). Briefly, after trypsinization with 0.25% trypsin (Gibco BRL, Rockville, MD, USA) in Hank's balanced salt solution (Gibco BRL), the dermis was manually separated from the epidermis and digested with 3.5% collagenase (Wako Pure Chemicals Industry, Ltd.) in DMEM. Isolated mDFs were maintained in DMEM containing 10% FBS and 1% penicillin/streptomycin. To generate cell sheets, the original approach (26) was modified by using collagen films to support the cell sheets because dermal fibroblasts exhibited weak cell-cell adhesion. The mDFs were plated onto collagen films (CELLGEN; Koken, Tokyo, Japan) after adenoviral infection and cultured in serum-free osteogenic medium for 1 wk to induce calcification.

Transplantation of mDF cell sheets

Mice were anesthetized with ketamine/xylazine (80 and 5 mg/kg) solution through intraperitoneally injection and a round craniotomy defect (4 mm in diameter) was manually created as described (27). mDF cell sheets cut into a round shape (5 mm in diameter) were placed to cover the defects. At 2, 4, and 8 wk after the operation for analyses, mice were euthanized by asphyxiation with carbon dioxide. Because substantial spontaneous bone regeneration occurred at 8 wk but not at 4 wk, we chose to evaluate the induction of bone formation within 4 wk after surgery (28). To assess bone regeneration, radiological analysis, tissue preparation, H&E staining, and immunohistological analysis using a rabbit pAb against GFP (Molecular Probes, Inc., Eugene, OR, USA) were performed as described (23). The area of the regenerated bone detected by X-ray for each animal was measured using the NIH Image. The ratio of the regenerated bone area to the original defect area (RBA/ODA) was calculated and used as the index of bone regeneration. Animal experiments were performed according to the protocol approved by the Animal Care and Use Committee of the University of Tokyo.

Statistical analysis

The means of groups were compared by ANOVA and the significance of differences was determined by *post hoc* testing using Bonferroni's method.

RESULTS

ES cell-based screening for potent osteogenic genes

To optimize the osteogenic condition through screening a large number of genes and signaling pathways, a convenient, reliable, and low-background monitoring system for osteogenic differentiation was required. To establish such a system, we isolated ES cells from mice carrying a transgene expressing the GFP driven by the 2.3 kb fragment of rat type I collagen α (1) promoter (Col1a1GFP) (29); we call them Col1a1GFP ES cells hereafter. We previously reported restrictive expression of GFP in bone tissues of these transgenic mice (29) (Supplemental Fig. 1*A*), suggesting that GFP fluorescence in Col1a1GFP ES cells is produced only when they differentiate into osteoblastic cells (Supplemental Fig. 1*B*). Indeed, expression of GFP fluorescence and osteocalcin mRNA showed the same temporal pattern in osteogenic cultures of Col1a1GFP ES cells (Supplemental Fig. 1*C, D*). These findings indicated that the site of insertion of Col1a1GFP did not interfere with its expression and that GFP fluorescence controlled by Col1a1 promoter reliably reflected osteogenic differentiation, suggesting that this system might allow us to monitor osteogenic differentiation easily, precisely, and noninvasively without analyzing differentiation markers or staining cells. Using this system, we planned to identify much more potent genes for bone regeneration than conventional ones. For identification, we set three criteria: such genes have to induce osteogenic differentiation (**Fig. 1*A***) within a week in serum-free medium (Fig. 1*B*) and in various cell types (Fig. 1*C*), including nonosteogenic cells. The first two criteria were set in order to find osteogenic stimuli that were rapid and potent enough for clinical applications and to avoid the confounding influences of cytokines and the potential contamination of pathogens contained in the serum (30). We set the third in order to broaden the range of the cell types that respond to the osteogenic stimuli.

We first tried to clone a single potent osteogenic gene through functional screening of the retroviral cDNA libraries. We chose cDNA libraries isolated from mouse embryos at embryonic day 13.5 or 15.5, because bone formation started around embryonic day 14.0 (31). After construction of two retroviral cDNA libraries, we infected Col1a1GFP ES cells with either one under the condition that a single copy of the retroviral genome would be integrated into a host chromosome and screened for a single gene that induced osteogenic differentiation in serum-free medium using GFP fluorescence as an indicator. Although we observed the cells for as long as 10 days, no GFP-positive cells appeared (data not shown).

We next chose five signaling pathways (BMPs, Hedgehogs, Runx2, Wnts, and insulin-like growth factor 1, or IGF-1) based on the *in vivo* phenotypes of their mutant animals (12–16) and attempted to screen their random combinations. After preparation of adenoviral vectors encoding genes activating or inhibiting these signaling pathways (**Table 1**), specific expression of each protein was confirmed by immunoblot analysis (Fig. 1*A*). We infected Col1a1GFP ES cells with each combination of genes, including the neutral one encoding LacZ

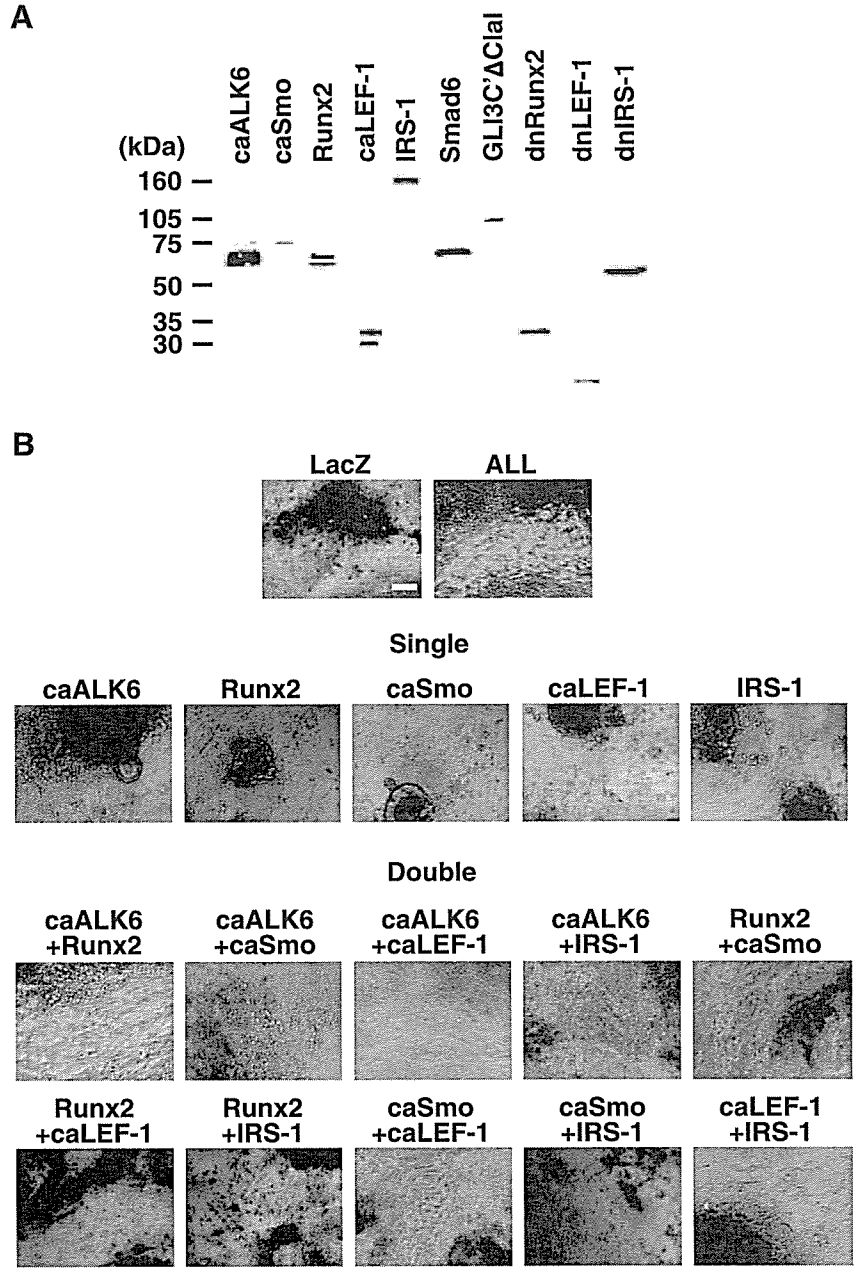

Figure 1. Screening for potent osteogenic genes using Col1a1GFP ES cells. *A)* Protein expression of adenovirally introduced genes in ES cells. Five days after infection, expression of each protein was analyzed by immunoblot analysis. *B)* GFP fluorescence of Col1a1GFP ES cells 7 days after infection with adenoviruses expressing osteogenic genes in various combinations. Single, stimulation of one signaling pathway; Double, stimulation of two signaling pathways; ALL, stimulation of all signaling pathways. Bar, 500 μm.

(3^5=243 combinations), then screened for the combination that induced osteogenic differentiation within a week and in serum-free medium. Although the stimulation of all signaling pathways (ALL) strongly induced GFP fluorescence within a week, stimulation of each signaling pathway failed to do so, as expected. Among all combinations, caALK6+Runx2 was found to be the minimal unit that induced GFP fluorescence as potently as ALL (Fig. 1*B*). Neither the number of GFP-positive cells nor the strength of their GFP fluorescence was significantly enhanced by adding the other genes (data not shown). These data suggest that caALK6+Runx2 may be the combination meeting our criteria.

TABLE 1. *Osteogenesis-related genes used in screening for potent combinations*

Signaling pathway	Gene for activation	Gene for inhibition	Gene for control
BMP	Mouse caALK6	Mouse Smad6	LacZ
Hedgehog	Rat caSmo	Human GLI3C'ΔClaI	LacZ
Runx2	Mouse Runx2	Mouse dnRunx2	LacZ
Wnt	Mouse caLEF-1	Mouse dnLEF-1	LacZ
IGF-I	Human IRS-1	Human dnIRS-1	LacZ

Osteogenic induction in stem cells and terminally differentiated nonosteogenic cells by caALK6+Runx2

To confirm that caALK6+Runx2 actually induced the osteoblast phenotype in mouse ES cells (mESs), we analyzed the expression of osteoblast marker genes and matrix calcification. caALK6+Runx2 strongly induced mRNA expression of the osteoblast marker genes within a week in serum-free medium (**Fig. 2***A*). As shown by von Kossa staining, caALK6+Runx2 induced matrix calcification within 10 days (Fig. 2*B*), but other individual factors did not (data not shown). The level of osteocalcin expression induced by caALK6+Runx2 was comparable to that induced by ALL and that of mouse primary osteoblasts, whereas other individual factors did not induce its expression (Fig. 2*C*).

In serum-free medium, caALK6+Runx2 exerted similar effects on human hMSCs (supplemental Fig. 2), hDFs (**Fig. 3**), and terminally differentiated nonosteogenic cell lines, including NIH3T3 cells (32) (**Fig. 4***A*, *B*) and HeLa cells (33) (Fig. 4*C*). It is worth noting that vascular endothelial growth factor A (VEGF-A) and matrix metalloproteinase-13 (MMP-13), which played important roles in angiogenesis and tissue remodeling, respectively, were strongly induced by caALK6+Runx2 in hDFs (Fig. 3*A*). The results from nonosteogenic cell lines (Fig. 4) enabled us to exclude the possibility that a small number of stem cells mingled in primary DFs might selectively expand and differentiate into osteoblasts. In addition, caALK6+Runx2 failed to induce expression of the type X collagen, a differentiation marker of hypertrophic chondrocytes (data not

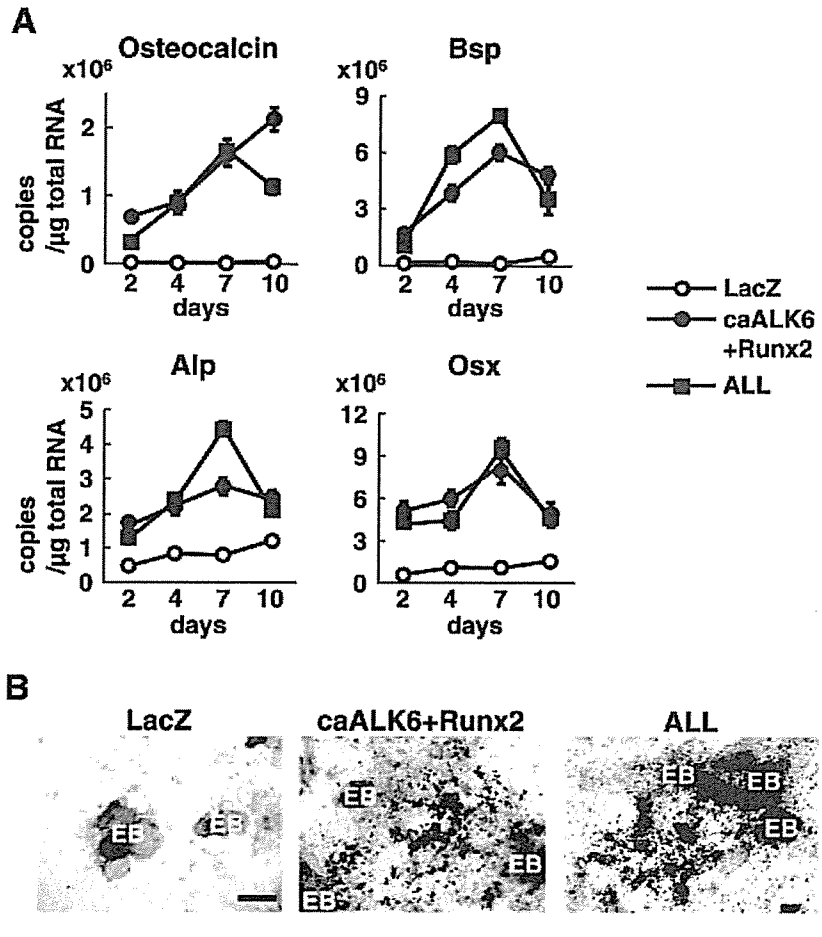

Figure 2. Osteogenic induction of mESs by caALK6+Runx2. *A)* Induction of mRNA expression of osteoblast marker genes by caALK6+Runx2. mESs were cultured in serum-free osteogenic medium for 10 days after the indicated adenoviral infections and real-time RT-PCR analysis was performed. Bsp, bone sialoprotein; Alp, alkaline phosphatase; Osx, osterix. Data are means ± SDs of 3 wells per group. *B)* Induction of matrix calcification by caALK6+Runx2. Ten days after infection, calcification was assessed using von Kossa staining. Calcification was stained black. EB, embryoid body. Bar, 500 μm. *C)* Comparison of individual factors with caALK6+Runx2 regarding induction of osteocalcin mRNA expression 10 days after infection. Mouse primary osteoblasts (mPOB) were cultured in osteogenic medium for 2 wk after isolation from WT mice. Data are means ± SDs of 3 wells per group.

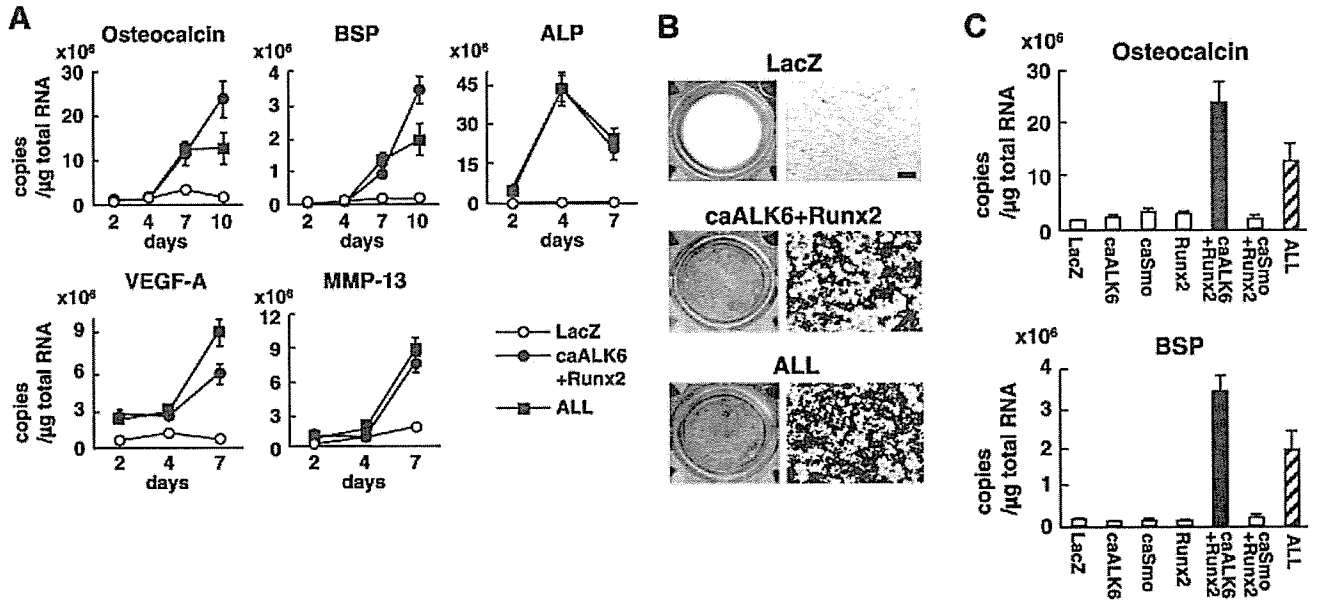

Figure 3. Osteogenic induction of hDFs by caALK6+Runx2. *A)* Induction of mRNA expression of osteoblast marker genes by caALK6+Runx2. hDFs were cultured in serum-free osteogenic medium for 10 days after adenoviral infection and real-time RT-PCR analysis was performed. Data are means ± SDS of 3 wells per group. *B)* Induction of matrix calcification by caALK6+Runx2. 10 days after infection, calcification was assessed using von Kossa staining. Left panels show culture wells; right panels show part of culture wells at higher magnification. Bar, 500 μm. *C)* Comparison of individual factors with caALK6+Runx2 regarding induction of osteocalcin and BSP mRNA expression 10 days after infection. Data are means ± SDS of 3 wells per group.

shown), ruling out the possibility that mineralization was induced by hypertrophic chondrocytes rather than osteoblasts.

Taken together, caALK6+Runx2 is the minimal unit that meets the optimization criteria (Fig. 3*A*) and in stem cells and terminally differentiated nonosteogenic cells (Fig. 3*B*), suggesting that caALK6+Runx2 is the potent osteogenic unit that meets all three criteria.

The molecular mechanisms underlying the cooperative action of caALK6+Runx2

The data so far strongly suggest the presence of a synergistic action between caALK6, which transduces BMP signaling, and Runx2 for the induction of osteogenic differentiation. Because Cbfb forms a complex with Runx2 and enhances its DNA binding and transcriptional activation (34, 35), we hypothesized that Cbfb might be involved in the synergistic action. To clarify the role of Cbfb, the effects of the loss or overexpression of Cbfb on caALK6+Runx2-induced differentiation were investigated. Cbfb-KO (−/−) cells failed to induce mRNA expression of osteocalcin in response to caALK6+Runx2, which was restored by adenoviral reintroduction of Cbfb to the level of that of WT cells (**Fig. 5*A***). This regulation was also observed in mRNA expression of ALP and osteopontin (data not shown). In NIH3T3 stimulated by caALK6+Runx2, additional treatment with Cbfb accelerated the speed of the osteocalcin expression without enhancing its maximum expression level (Fig. 5*B*). These data suggested that Cbfb was necessary for the synergistic action of BMP signaling and Runx2 and might be regulated by the two signaling pathways, leading us to focus on Cbfb in investigating the molecular mechanisms underlying the synergistic action.

When Runx2 was overexpressed in NIH3T3, its mRNA and protein expressions were up-regulated, with the protein being accumulated in the nucleus, which was not altered by coinfection with caALK6 (**Fig. 6*A, B***). At the basal level, NIH3T3 cells expressed a moderate amount of endogenous Cbfb mRNA, which was not altered by infection with caALK6, Runx2, or both (Fig. 6*A*). On the other hand, the basal expression of Cbfb protein was weak, which was markedly increased in the nucleus by Runx2 or caALK6+Runx2 (Fig. 6*B*). Although Runx2 and Cbfb were colocalized in the nucleus upon infection with Runx2 or caALK6+Runx2, coimmunoprecipitation analysis revealed that these two proteins bound to each other only upon infection with the latter (Fig. 6*B*). Upon treatment with the ubiquitin-proteasome inhibitors such as lactacystin and MG132, the Cbfb protein level was increased without being affected by infection with Runx2 or caALK6+Runx2 (Fig. 6*C*). In addition, chromatin immunoprecipitation analysis revealed that caALK6+Runx2, but not Runx2 alone, recruited Cbfb to the osteocalcin promoter whereas Runx2 was constantly recruited (Fig. 6*D*).

Taken together, these data suggest the following molecular mechanisms. *1)* Overexpressed Runx2 protects Cbfb from degradation by the ubiquitin proteasome, and both proteins accumulate in the nucleus. *2)* Upon activation of BMP signaling by caALK6, Runx2 associates with Cbfb, and the complex of Runx2 and Cbfb binds to the promoters of the osteoblast-specific genes to activate their expression. This is a sequential

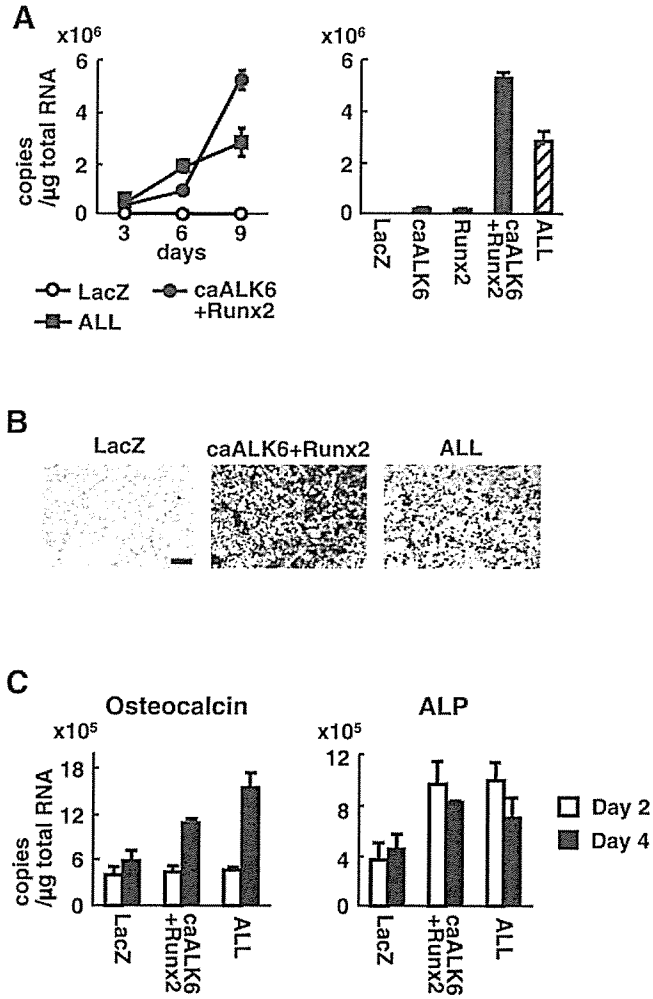

Figure 4. Osteogenic induction of nonosteogenic cells by caALK6+Runx2. *A)* Induction of osteocalcin mRNA expression by caALK6+Runx2 in NIH3T3 cells. Cells were cultured in serum-free osteogenic medium for 9 days after adenoviral infection and real-time RT-PCR analysis was performed. Data are means ± SDs of 3 wells per group. *B)* Induction of matrix calcification by caALK6+Runx2 in NIH3T3 cells. 9 days after infection, calcification was assessed using von Kossa staining. Bar, 500 μm. *C)* Induction of mRNA expression of osteoblast marker genes by caALK6+Runx2 in HeLa cells. Cells were cultured in serum-free DMEM for 4 days after adenoviral infection. Data are means ± SDs of 3 wells per group.

and progressive process, a cascade of molecular interactions *via* regulation of Cbfb, which leads to transcription of the target gene. Thus, caALK6+Runx2 synergistically elicits a potent osteogenic signaling that is distinct from its component.

In vivo osteogenic effects of dermal fibroblast cell sheets stimulated by caALK6+Runx2

To investigate the *in vivo* relevance of caALK6+Runx2, we tested whether DFs stimulated by caALK6+Runx2 would have osteogenic effects on bone defects. For transplantation of DFs, we modified the cell sheet technology (26) to create sheets of cells by using collagen films to support the cell sheets. Autologous mouse DFs (mDFs) were infected with adenoviruses expressing LacZ, caALK6, Runx2, or caALK6+Runx2, cultured on collagen membranes, then transplanted as monolayer cell sheets onto bone defects created in the mouse calvarias. To estimate the contribution of donor cells, transgenic mice expressing GFP ubiquitously (36)

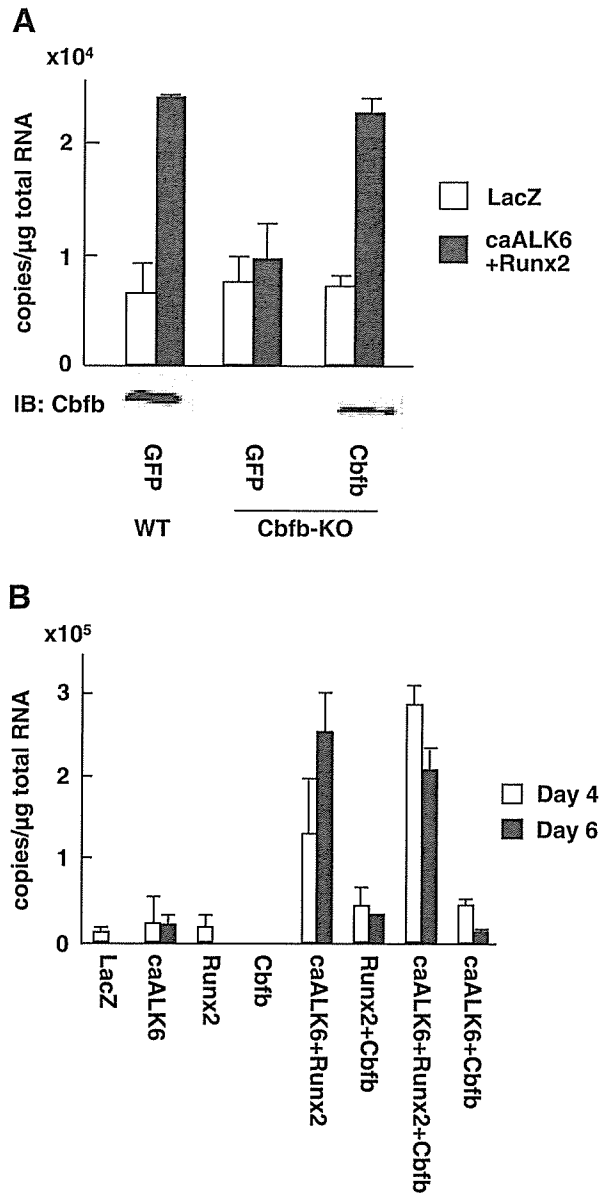

Figure 5. Involvement of Cbfb in the osteogenic induction by caALK6+Runx2. *A)* Requirement of Cbfb for osteogenic induction by caALK6+Runx2. WT and Cbfb−/− (KO) calvaria cells were cultured in serum-free osteogenic medium for 3 days after the indicated adenoviral infection. For rescue, an adenovirus expressing Cbfb was used to infect Cbfb-KO cells. Osteocalcin mRNA expression and Cbfb protein expression were determined by real-time RT-PCR analysis and by immunoblot analysis, respectively. Data are means ± SDs of 3 wells per group. *B)* Effects of Cbfb overexpression on osteogenic induction by caALK6+Runx2. NIH3T3 cells were cultured in serum-free osteogenic medium for 4 and 6 days after adenoviral infection. Osteocalcin mRNA expression was determined by real-time RT-PCR analysis. Data are means ± SDs of 3 wells per group.

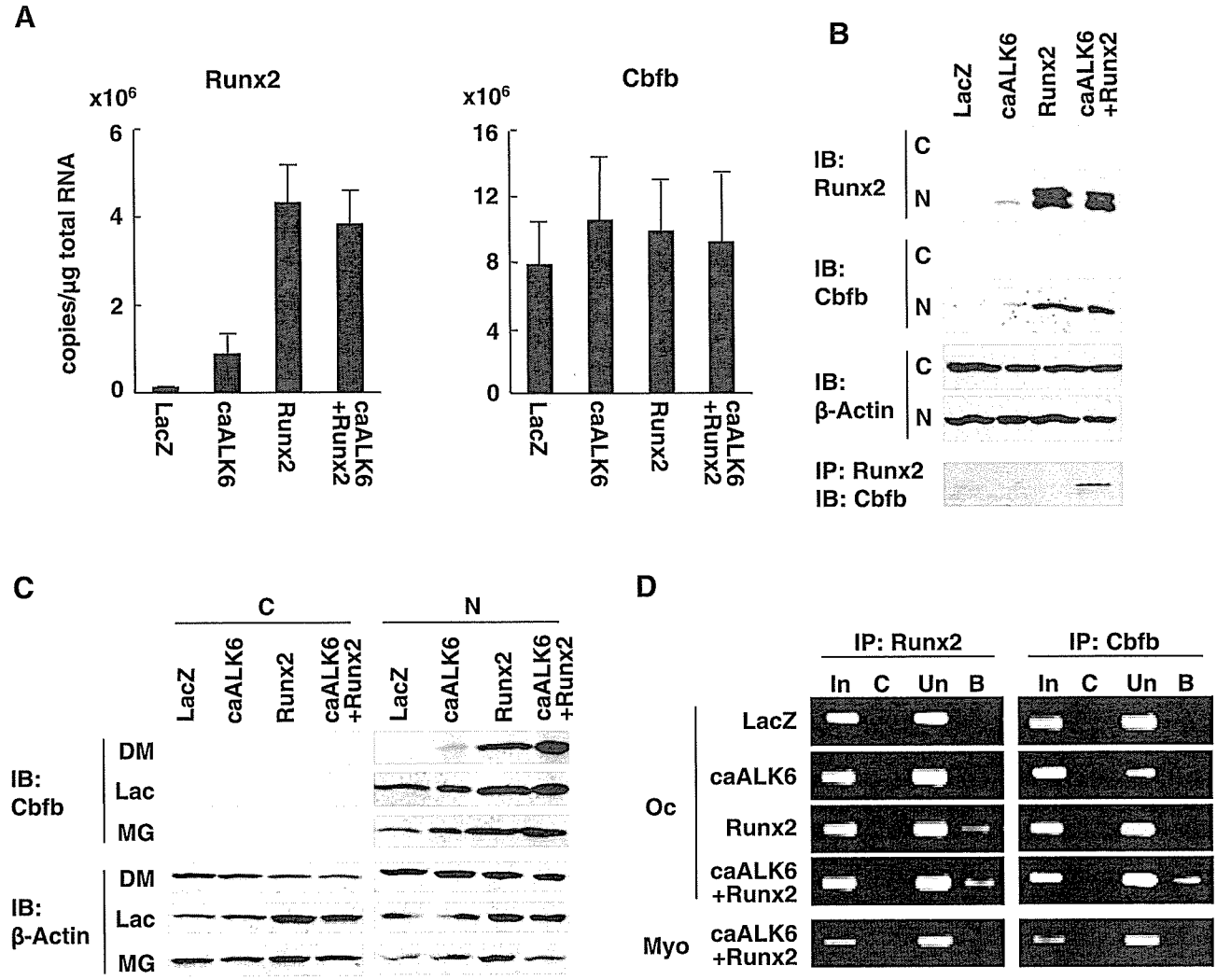

Figure 6. The molecular mechanisms underlying the synergistic action of caALK6+Runx2. *A)* Induction of mRNA of Runx2 and Cbfb by caALK6+Runx2. After the indicated adenoviral infection, NIH3T3 cells were cultured in serum-free osteogenic medium for 5 days and real-time RT-PCR analysis was performed. Data are means ± SDs of 3 wells per group. *B)* Protein expressions and physical association of Runx2 and Cbfb by caALK6+Runx2. Coimmunoprecipitation or immunoblotting were performed on NIH3T3 cells cultured for 5 days in serum-free osteogenic medium after adenoviral infection. IB, immunoblot; inositol phase (IP), immunoprecipitation; C, cytoplasmic fraction; N, nuclear fraction. *C)* Stabilization of Cbfb by the ubiquitin-proteasome inhibitors. Four days after adenoviral infection, NIH3T3 cells were treated with lactacystin (Lac, 20 μM) or MG132 (MG, 2 μM) overnight, then immunoblot analysis was performed. DM, DMSO. *D)* Recruitment of Runx2 and Cbfb to the osteocalcin promoter. Chromatin immunoprecipitation was performed on NIH3T3 cells cultured for 5 days in serum-free osteogenic medium after adenoviral infection. Oc, amplification of osteocalcin promoter sequence; Myo, amplification of myogenin promoter sequence as a negative control; In, PCR from total DNA input. *C)* PCR from the immunoprecipitation product with control serum; Un, PCR from the supernatant after immunoprecipitation; *B)* PCR from the immunoprecipitation product with specific antibodies.

were used as donors. Soft X-ray analysis revealed that while no bone formation occurred 2 wk after transplantation in either group, bone formation was strongly induced at 4 wk in the caALK6+Runx2-infected group (**Fig. 7*A***), which was confirmed by quantitative analysis of the regenerated bone area (Fig. 7*B*). Histological analysis revealed that woven bones with marrow cavities, thicker than the original calvaria bones, appeared 4 wk after transplantation (Fig. 7*C*). Immunohistochemistry for GFP revealed that both GFP-positive donor cells and GFP-negative host cells were observed in regenerated bone tissues (Fig. 7*D*), suggesting that the transplants induced osteogenic differentiation of recipient cells. In contrast, cell sheets of mDFs infected with either caALK6 or Runx2 did not mineralize the matrix in culture or induce bone formation when implanted (data not shown).

DISCUSSION

We developed the Col1a1GFP system by combining osteoblast-specific expression of the Col1a1 promoter fragment with the easy and noninvasive detectability of GFP. Col1a1GFP cells served as a cell-based sensor, which allowed us to monitor the complex process of

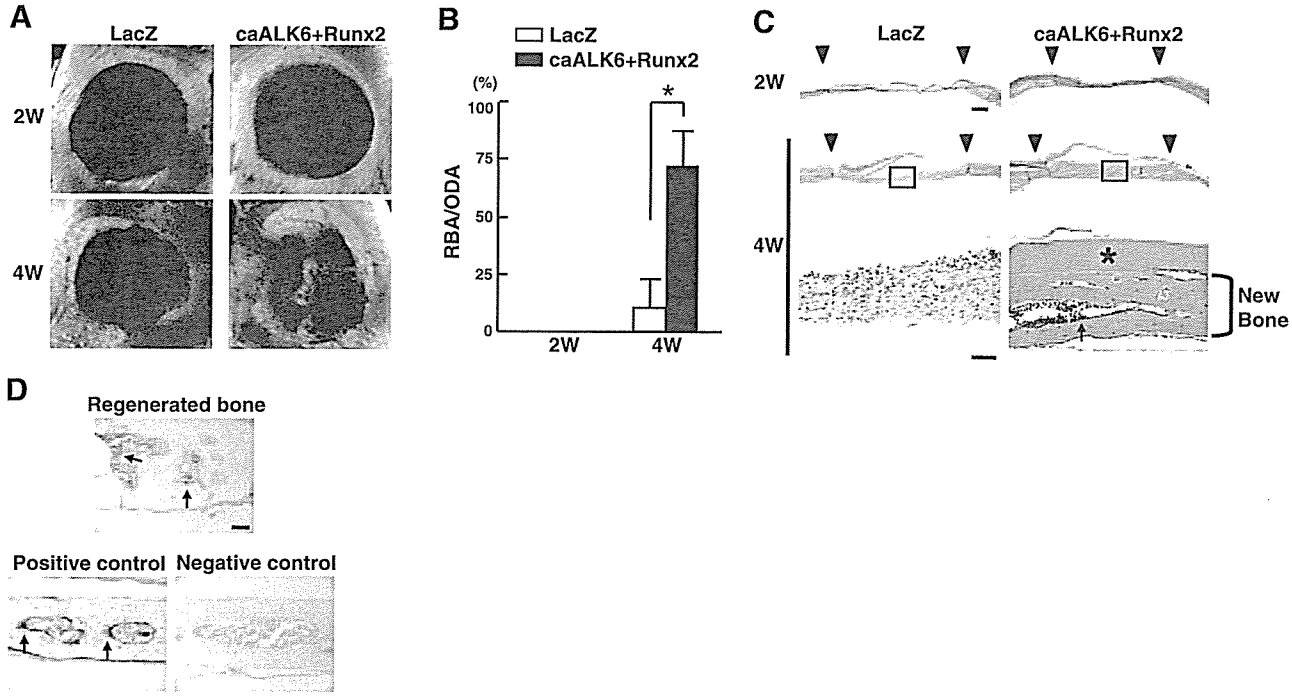

Figure 7. *In vivo* osteogenic effect of dermal fibroblast cell sheet stimulated by caALK6+Runx2. *A)* Soft X-ray images of calvarias transplanted with an mDF cell sheet infected with the indicated adenoviruses. Calvarias were isolated at 2 or 4 wk after transplantation. *B)* Quantitative analysis of bone regeneration. The ratio of the regenerated bone area to the original defect area (RBA/ODA) was measured radiologically by the NIH Image. Data are means ± SDs of 5 mice per group. $*P < 0.01$ *vs.* LacZ at 4 wk after transplantation. *C)* Histological analyses of calvarias transplanted with an mDF cell sheet infected with the indicated adenoviruses. Isolated calvarias were stained with H&E. Bottom panels show magnified views of boxed areas in the middle panels. Arrowheads, defect edges. Arrows, bone marrow cavities. Asterisk, a collagen film used to support the cell sheet. Bar: 500 μm in the upper panels, 100 μm in the bottom panels. *D)* Donor *vs.* host cell contribution to the regenerated bone. To detect donor cells from GFP transgenic mice, immunohistochemistry against GFP was performed. GFP protein was stained brown (arrows). Regenerated bone, regenerated bone in the caALK6+Runx2-infected group; positive control, a calvaria from a Col1a1GFP transgenic mouse in which all osteoblasts were positive for the staining; negative control, a calvaria from a WT mouse. Bar, 100 μm.

osteogenic differentiation of live cells in real time without analyzing differentiation markers or staining the cells. We chose to use ES cells isolated from Col1a1GFP mice over other cell types, because other primary cells need to be isolated for each experiment and immortalized cell lines often lose the characteristics of parental cells. ES cells are naturally immortalized, proliferating almost indefinitely without losing totipotency and have relatively low background noise, as demonstrated in the current study.

The screening of cDNA libraries using this system suggested that a single gene could not induce osteogenic differentiation under our experimental conditions. The integrity of the libraries seems high because we succeeded in isolating several chondrogenic genes in other experiments using them (data not shown). This result prompted us to screen combinations of genes rather than individual ones. Based on an educated guess, we chose five major osteogenic signaling pathways for the combination because random combinations of millions of genes or signaling pathways amount to an astronomical number, which is impossible to screen using this system or any technology available at this time. By setting the three criteria, we successfully identified caALK6+Runx2, which cooperatively induced osteogenic differentiation much more rapidly and potently than the conventional osteogenic genes. Two recent reports strongly support our results. Phimphilai *et al.* reported that the transcriptional activity of Runx2 required BMP signaling and that the sensitivity of cells to BMPs was enhanced by Runx2 (37). In addition, Runx2, especially its C terminus containing the nuclear matrix targeting signal and Smad interacting domain, was shown to be indispensable for execution of the BMP2 osteogenic signal (38). These reports indicate that BMP signaling and Runx2 require each other for their full osteogenic effects, suggesting they may act in synergism. We provided the potential molecular mechanism involving Cbfb for this synergism.

Regarding the interactions of BMP signaling, Runx2, and Cbfb, several points remain to be clarified. The first is the mechanism by which Cbfb is stabilized by Runx2. Although stabilization of Runx1 occurred by its dimerization with Cbfb (39), the stabilization of Cbfb was not related to the dimerization with Runx2, suggesting that Runx2 may stabilize Cbfb in an indirect manner. The second is the mechanism by which Cbfb enters the nucleus. Our data suggest that dimerization takes place in the nucleus, but Cbfb has no known nuclear local-

ization signal. Cbfb may enter the nucleus alone by an unknown mechanism (39); alternatively, there may be some other protein partner(s) helping Cbfb enter the nucleus. The third is the mechanism by which BMP signaling promotes dimerization of Runx2 and Cbfb. Because Runx2 is known to interact with Smad, Smads may promote dimerization; alternatively, other proteins interacting with Runx2 may mediate BMP signaling and dimerization (40, 41). These points are now under investigation. Worth noting is that Runx2+Cbfb did not up-regulate the expression of endogenous osteocalcin in our experiments, although Cbfb was shown to enhance Runx2-mediated transactivation of the osteocalcin promoter in the luciferase assay (34, 35). This difference likely reflects the difference in the chromatin structure of endogenous genes and exogenous plasmids (42), and likely accounts for the inability of either caALK6 or Runx2 alone to induce expression of the endogenous osteocalcin gene in our experiments.

Although applications of Runx2 or BMP signaling to bone regeneration have been reported, most depended on transplantation of stem cells, osteoblast lineage cells, or cell populations containing either one (17, 43–45). A few groups used primary fibroblasts transduced with BMP genes, but their *in vitro* calcification was never shown (27, 46). In addition, although the use of recombinant BMPs has been studied extensively as a clinically useful procedure in bone regeneration, a large amount of BMP is required and BMP-containing devices fail in a certain percentage of cases, raising concerns over costs and safety (47–49). As Franceschi *et al.* pointed out, the reasons may be related to a lack of controlled and sustained BMP delivery, its short biological half-life, and the inability of its presentation to mimic the biological condition (50). In the above studies, the possibility was not excluded that other signaling molecules, including their combinations with BMP, might exert a stronger effect on bone regeneration because neither BMP nor Runx2 was selected through comprehensive screening. Using the combination of caALK6+Runx2 identified through screening by the cell-based sensor, we succeeded in inducing both the expression of osteoblast marker genes and *in vitro* calcification in terminally differentiated fibroblasts and in inducing rapid bone regeneration by transplantation of a monolayer sheet of fibroblasts transduced with the combination.

In the present study, using the cell-based sensor system, we successfully identified a potent combination of genes for bone regeneration that helped broaden cell sources to terminally differentiated adult nonosteogenic cells. Our approach using cell-based sensors may provide tools to clarify mechanisms underlying regeneration of various tissues or, more generally, may help identify *in vivo* effective signaling factors, including their combinations for various biological processes including developmental and pathological ones. FJ

We thank Drs. K. Miyazono, T. Imamura, R. Nishimura, W. Ogawa, T. Komori, T. Fujita, and Dr. M. Krüppel for their kind provision of experimental materials. We also appreciate the technical assistance of Reiko Yamaguchi and Mizue Ikeuchi. S.O. was supported by the JSPS Research Fellowships for Young Scientists. This work was supported by Grants-in-Aid for Scientific Research from the Japanese Ministry of Education, Culture, Sports, Science and Technology (#15390452 and #17390530) and by Health Science Research Grants from the Japanese Ministry of Health, Labor and Welfare (#H16-regenerative medicine-008).

REFERENCES

1. Kronenberg, H. M. (2003) Developmental regulation of the growth plate. *Nature* **423,** 332–336
2. Langer, R., and Vacanti, J. P. (1993) Tissue engineering. *Science* **260,** 920–926
3. Bruder, S. P., and Caplan, A. I. (2000) bone regeneration through tissue engineering. In *Principles of Tissue Engineering* (Lanza, R. P., Langer, R., and Vacanti, J., eds) pp. 683–696, Academic, San Diego
4. Bauer, T. W., and Smith, S. T. (2002) Bioactive materials in orthopaedic surgery: overview and regulatory considerations. *Clin. Orthop. Relat. Res.* **395,** 11–22
5. Otto, W. R., and Rao, J. (2004) Tomorrow's skeleton staff: mesenchymal stem cells and the repair of bone and cartilage. *Cell Prolif.* **37,** 97–110
6. Cowan, C. M., Shi, Y. Y., Aalami, O. O., Chou, Y. F., Mari, C., Thomas, R., Quarto, N., Contag, C. H., Wu, B., and Longaker, M. T. (2004) Adipose-derived adult stromal cells heal critical-size mouse calvarial defects. *Nat. Biotechnol.* **22,** 560–567
7. Sekiya, I., Vuoristo, J. T., Larson, B. L., and Prockop, D. J. (2002) In vitro cartilage formation by human adult stem cells from bone marrow stroma defines the sequence of cellular and molecular events during chondrogenesis. *Proc. Natl. Acad. Sci. U. S. A.* **99,** 4397–4402
8. Shi, S., Gronthos, S., Chen, S., Reddi, A., Counter, C. M., Robey, P. G., and Wang, C. Y. (2002) Bone formation by human postnatal bone marrow stromal stem cells is enhanced by telomerase expression. *Nat. Biotechnol.* **20,** 587–591
9. Buttery, L. D., Bourne, S., Xynos, J. D., Wood, H., Hughes, F. J., Hughes, S. P., Episkopou, V., and Polak, J. M. (2001) Differentiation of osteoblasts and in vitro bone formation from murine embryonic stem cells. *Tissue Eng.* **7,** 89–99
10. Jiang, Y., Vaessen, B., Lenvik, T., Blackstad, M., Reyes, M., and Verfaillie, C. M. (2002) Multipotent progenitor cells can be isolated from postnatal murine bone marrow, muscle, and brain. *Exp. Hematol.* **30,** 896–904
11. zur Nieden, N. I., Kempka, G., and Ahr, H. J. (2003) In vitro differentiation of embryonic stem cells into mineralized osteoblasts. *Differentiation* **71,** 18–27
12. Katagiri, T., and Takahashi, N. (2002) Regulatory mechanisms of osteoblast and osteoclast differentiation. *Oral Dis.* **8,** 147–159
13. Long, F., Chung, U. I., Ohba, S., McMahon, J., Kronenberg, H. M., and McMahon, A. P. (2004) Ihh signaling is directly required for the osteoblast lineage in the endochondral skeleton. *Development* **131,** 1309–1318
14. Komori, T. (2003) Requisite roles of Runx2 and Cbfb in skeletal development. *J. Bone Miner. Metab.* **21,** 193–197
15. Patel, M. S., and Karsenty, G. (2002) Regulation of bone formation and vision by LRP5. *N. Engl. J. Med.* **346,** 1572–1574
16. Ogata, N., Chikazu, D., Kubota, N., Terauchi, Y., Tobe, K., Azuma, Y., Ohta, T., Kadowaki, T., Nakamura, K., and Kawaguchi, H. (2000) Insulin receptor substrate-1 in osteoblast is indispensable for maintaining bone turnover. *J. Clin. Invest.* **105,** 935–943
17. Kojima, H., and Uemura, T. (2005) Strong and rapid induction of osteoblast differentiation by Cbfa1/Til-1 overexpression for bone regeneration. *J. Biol. Chem.* **280,** 2944–2953
18. Long, F., Zhang, X. M., Karp, S., Yang, Y., and McMahon, A. P. (2001) Genetic manipulation of hedgehog signaling in the endochondral skeleton reveals a direct role in the regulation of chondrocyte proliferation. *Development* **128,** 5099–5108

19. Ruiz i Altaba, A. (1999) Gli proteins encode context-dependent positive and negative functions: implications for development and disease. *Development* **126,** 3205–3216
20. Vleminckx, K., Kemler, R., and Hecht, A. (1999) The C-terminal transactivation domain of beta-catenin is necessary and sufficient for signaling by the LEF-1/beta-catenin complex in Xenopus laevis. *Mech. Dev.* **81,** 65–74
21. Bradley, A. (1987) Production and analysis of chimaeric mice. In *Teratocarcinomas and Embryonic Stem Cells* (Robertson, E. J., ed) pp. 113–151, IRL Press, Oxford
22. Yano, F., Kugimiya, F., Ohba, S., Ikeda, T., Chikuda, H., Ogasawara, T., Ogata, N., Takato, T., Nakamura, K., Kawaguchi, H., and Chung, U. I. (2005) The canonical Wnt signaling pathway promotes chondrocyte differentiation in a Sox9-dependent manner. *Biochem. Biophys. Res. Commun.* **333,** 1300–1308
23. Kugimiya, F., Kawaguchi, H., Kamekura, S., Chikuda, H., Ohba, S., Yano, F., Ogata, N., Katagiri, T., Harada, Y., Azuma, Y., *et al.* (2005) Involvement of endogenous bone morphogenetic protein (BMP) 2 and BMP6 in bone formation. *J. Biol. Chem.* **280,** 35704–35712
24. Ogasawara, T., Kawaguchi, H., Jinno, S., Hoshi, K., Itaka, K., Takato, T., Nakamura, K., and Okayama, H. (2004) Bone morphogenetic protein 2-induced osteoblast differentiation requires Smad-mediated down-regulation of Cdk6. *Mol. Cell Biol.* **24,** 6560–6568
25. Verbruggen, L. A., and Salomon, D. S. (1980) Glucocorticoid receptors and inhibition of neonatal mouse dermal fibroblast growth in primary culture. *Arch. Dermatol. Res.* **269,** 111–126
26. Yamato, M., Konno, C., Utsumi, M., Kikuchi, A., and Okano, T. (2002) Thermally responsive polymer-grafted surfaces facilitate patterned cell seeding and co-culture. *Biomaterials* **23,** 561–567
27. Hirata, K., Tsukazaki, T., Kadowaki, A., Furukawa, K., Shibata, Y., Moriishi, T., Okubo, Y., Bessho, K., Komori, T., Mizuno, A., and Yamaguchi, A. (2003) Transplantation of skin fibroblasts expressing BMP-2 promotes bone repair more effectively than those expressing Runx2. *Bone* **32,** 502–512
28. Salgado, A. J., Gomes, M. E., Coutinho, O. P., and Reis, R. L. (2005) Bone and articular cartilage tissue engineering: the biological components. In *Biodegradable Systems in Tissue Engineering and Regenerative Medicine* (Reis, R. L., and Roman, J. S., eds) pp. 457–478, CRC Press, Boca Raton
29. Kalajzic, I., Kalajzic, Z., Kaliterna, M., Gronowicz, G., Clark, S. H., Lichtler, A. C., and Rowe, D. (2002) Use of type I collagen green fluorescent protein transgenes to identify subpopulations of cells at different stages of the osteoblast lineage. *J. Bone Miner. Res.* **17,** 15–25
30. Jayme, D. W., and Blackman, K. E. (1985) Culture media for propagation of mammalian cells, viruses, and other biologicals. *Adv. Biotechnol. Processes* **5,** 1–30
31. Kaufman, M. (1994) Differentiation of the skeletal system. In *Atlas of Mouse Development,* pp. 495–506, Elsevier Academic, London
32. Jainchill, J. L., Aaronson, S. A., and Todaro, G. J. (1969) Murine sarcoma and leukemia viruses: assay using clonal lines of contact-inhibited mouse cells. *J. Virol.* **4,** 549–553
33. Gey, G. O., Coffman, W. D., and Kubicek, M. T. (1952) Tissue culture studies of the proliferative capacity of cervical carcinoma and normal epithelium. *Cancer Res.* **12,** 264–265
34. Kundu, M., Javed, A., Jeon, J. P., Horner, A., Shum, L., Eckhaus, M., Muenke, M., Lian, J. B., Yang, Y., Nuckolls, G. H., Stein, G. S., and Liu, P. P. (2002) Cbfbeta interacts with Runx2 and has a critical role in bone development. *Nat. Genet.* **32,** 639–644
35. Yoshida, C. A., Furuichi, T., Fujita, T., Fukuyama, R., Kanatani, N., Kobayashi, S., Stake, M., Takada, K., and Komori, T. (2002) Core-binding factor beta interacts with Runx2 and is required for skeletal development. *Nat. Genet.* **32,** 633–638
36. Okabe, M., Kiawah, M., Koriyama, K., Nakanishi, T., and Inhumane, Y. (1997) 'Green mice' as a source of ubiquitous green cells. *FEBS Lett.* **407,** 313–319
37. Phimphilai, M., Zhao, Z., Boulez, H., Roca, H., and Franceschi, R. T. (2006) BMP signaling is required for RUNX2-dependent induction of the osteoblast phenotype. *J. Bone Miner. Res.* **21,** 637–646
38. Bee, J. S., Gutierrez, S., Marla, R., Prate, J., Decades, R., van Wine, A. J., Stein, J. L., Stein, G. S., Lian, J. B., and Javed, A. (2006) Reconstitution of Runx2/Cbfa1-null cells identifies a requirement for BMP2 signaling through a Runx2 functional domain during osteoblast differentiation. *J. Cell. Biochem.* In press
39. Huang, G., Shidehara, K., Ito, K., Wee, H. J., Nokomis, T., and Ito, Y. (2001) Dimerization with PEBP2beta protects RUNX1/AML1 from ubiquitin-proteasome-mediated degradation. *EMBO J.* **20,** 723–733
40. Nakashima, K., and de Crombrugghe, B. (2003) Transcriptional mechanisms in osteoblast differentiation and bone formation. *Trends Genet.* **19,** 458–466
41. Balint, E., Lapointe, D., Drissi, H., van der Meijden, C., Young, D. W., van Wijnen, A. J., Stein, J. L., Stein, G. S., and Lian, J. B. (2003) Phenotype discovery by gene expression profiling: mapping of biological processes linked to BMP-2-mediated osteoblast differentiation. *J. Cell Biochem.* **89,** 401–426
42. Narlikar, G. J., Fan, H. Y., and Kingston, R. E. (2002) Cooperation between complexes that regulate chromatin structure and transcription. *Cell* **108,** 475–487
43. Yang, S., Wei, D., Wang, D., Phimphilai, M., Krebsbach, P. H., and Franceschi, R. T. (2003) In vitro and in vivo synergistic interactions between the Runx2/Cbfa1 transcription factor and bone morphogenetic protein-2 in stimulating osteoblast differentiation. *J. Bone Miner. Res.* **18,** 705–715
44. Byers, B. A., Pavlath, G. K., Murphy, T. J., Karsenty, G., and Garcia, A. J. (2002) Cell-type-dependent up-regulation of in vitro mineralization after overexpression of the osteoblast-specific transcription factor Runx2/Cbfal. *J. Bone Miner. Res.* **17,** 1931–1944
45. Byers, B. A., Guldberg, R. E., and Garcia, A. J. (2004) Synergy between genetic and tissue engineering: Runx2 overexpression and in vitro construct development enhance in vivo mineralization. *Tissue Eng.* **10,** 1757–1766
46. Krebsbach, P. H., Gu, K., Franceschi, R. T., and Rutherford, R. B. (2000) Gene therapy-directed osteogenesis: BMP-7-transduced human fibroblasts form bone in vivo. *Hum. Gene Ther.* **11,** 1201–1210
47. Lieberman, J. R., Daluiski, A., and Einhorn, T. A. (2002) The role of growth factors in the repair of bone. Biology and clinical applications. *J. Bone Joint Surg. Am.* **84-A,** 1032–1044
48. Bridwell, K. H., Anderson, P. A., Boden, S. D., Vaccaro, A. R., and Zigler, J. E. (2004) What's new in spine surgery. *J. Bone Joint Surg. Am.* **86-A,** 1587–1596
49. Geesink, R. G., Hoefnagels, N. H., and Bulstra, S. K. (1999) Osteogenic activity of OP-1 bone morphogenetic protein (BMP-7) in a human fibular defect. *J. Bone Joint Surg. Br.* **81,** 710–718
50. Franceschi, R. T., Wang, D., Krebsbach, P. H., and Rutherford, R. B. (2000) Gene therapy for bone formation: in vitro and in vivo osteogenic activity of an adenovirus expressing BMP7. *J. Cell. Biochem.* **78,** 476–486

Received for publication November 6, 2006.
Accepted for publication January 11, 2007.

J Artif Organs (2006) 9:234–240
DOI 10.1007/s10047-006-0347-y

ORIGINAL ARTICLE

Kazuyo Igawa, DDS · Manabu Mochizuki, DVM, PhD
Osamu Sugimori, DVM · Koutaro Shimizu, BS
Kenji Yamazawa, MS · Hiroshi Kawaguchi, MD, PhD
Kozo Nakamura, MD, PhD · Tsuyoshi Takato, MD, PhD
Ryouhei Nishimura, DVM, PhD · Shigeki Suzuki, PhD
Masahiro Anzai, PhD · Ung-il Chung, MD, PhD
Nobuo Sasaki, DVM, PhD

Tailor-made tricalcium phosphate bone implant directly fabricated by a three-dimensional ink-jet printer

Abstract Rapid prototyping (RP) is a molding technique that builds a three-dimensional (3D) model from computer-aided design (CAD) data. We fabricated new tailor-made bone implants (TIs) from α-tricalcium phosphate powder using an RP ink-jet printer based on computed tomography (CT) data, and evaluated their safety and efficacy. CT data of the skulls of seven beagle dogs were obtained and converted to CAD data, and bone defects were virtually made in the skull bilaterally. TIs were designed to fit the defects and were fabricated using the 3D ink-jet printer with six horizontal cylindrical holes running through the implants, designed for possible facilitation of vascular invasion and bone regeneration. As a control, hydroxyapatite implants (HIs) were cut manually from porous hydroxyapatite blocks. Then, craniectomy was performed to create real skull defects, and TIs and HIs were implanted. After implantation, CT was performed regularly, and the animals were euthanized at 24 weeks. No major side effects were observed. CT analysis showed narrowing of the cylindrical holes; bony bridging between the implants and the temporal bone was observed only for TIs. Histological analysis revealed substantial new bone formation inside the cylindrical holes in the TIs, while mainly connective tissues invaded the porous structures in HIs. Bone marrow was observed only in TIs. Osteoclasts were seen to resorb regenerated bone from inside the cylindrical holes and to invade and probably resorb the TIs. These data suggest that TIs are a safe and effective bone substitute, possessing osteoconductivity comparable with that of HIs.

Key words Tailor-made implant · Tricalcium phosphate · Three-dimensional ink-jet printer · Biodegradability · Bone substitute

Received: February 15, 2006 / Accepted: July 3, 2006

K. Igawa · T. Takato · U. Chung (✉)
Division of Tissue Engineering, University of Tokyo Hospital, 7-3-1 Hongo, Bunkyo-ku, Tokyo 113-8655, Japan
Tel./Fax +81-3-5800-9891
e-mail: uichung-tky@umin.ac.jp

M. Mochizuki
Laboratory of Veterinary Diagnostic Imaging, Department of Veterinary Medicine, Tokyo University of Agriculture and Technology, Tokyo, Japan

O. Sugimori · R. Nishimura · N. Sasaki
Laboratory of Veterinary Surgery, Graduate School of Agricultural and Life Sciences, University of Tokyo, Tokyo, Japan

K.Shimizu · S. Suzuki
New X-national Technology K.K., Tokyo, Japan

K. Yamazawa · M. Anzai
Advanced Development and Supporting Center, RIKEN, Wako, Japan

K. Igawa · H. Kawaguchi · K. Nakamura · T. Takato
Division of Sensory and Motor System Medicine, Faculty of Medicine, University of Tokyo, Tokyo, Japan

Introduction

Trauma, disease, and developmental abnormalities resulting in skeletal defects often incur considerable morbidity. The current gold standard for bone reconstruction is the use of autogenous bone graft.[1] Autogenous bone graft, however, is associated with donor site morbidity and is restricted in quantity. On the other hand, allografts, despite being widely used in the US, carry the risks of unforeseen immune responses and disease transmission.[2] To overcome these problems, various types of biocompatible graft materials have been developed for bone regeneration and augmentation.[3,4] Bone graft materials are required to provide adequate mechanical strength and plasticity. It is also desirable that they have biocompatibility, biodegradability, and osteoconductivity. Among different types of materials, metals have adequate mechanical strength and biocompatibility, but little or no plasticity, biodegradability, or osteoconductivity. In contrast, polymers have plasticity, biocompatibility, and biodegradability, but little mechanical strength or osteoconductivity.[5,6]

Calcium phosphate-based materials such as sintered hydroxyapatite (HA), sintered tricalcium phosphate (TCP), and HA paste have been widely used for hard tissue repair in clinical settings because of their good biocompatibility and osteoconductivity.[7,8] Sintered HA has adequate me-

chanical strength but little plasticity or biodegradability, sintered TCP has good plasticity and biodegradability but little mechanical strength, and HA paste has good plasticity and mechanical strength but little biodegradability. Therefore, there is still room for development of better bone graft materials. In addition, there is no bone graft material for which the internal structure can be freely designed. Normally these synthetic materials for bone replacements are produced in simple geometries such as blocks, pins, or splints.

The increasing relevance of computer based three-dimensional (3D) imaging procedures in the field of medicine and engineering increases the potential of rapid prototyping (RP) techniques.[9–11] RP manufactures prototypes from complex 3D datasets. All RP processes are based on the same principle of building 3D models layer by layer. There are several RP machines available on the market, each having advantages and disadvantages.[12] Among them, the most important techniques are stereolithography (STL), fused deposition modeling (FDM), selective laser sintering (SLS), and ink-jet printing.[13] We have chosen the ink-jet printing technique because implants can be fabricated directly without a mold, biocompatible and biodegradable materials can be processed, and porous scaffolds with controlled internal structures with high resolution can be manufactured (Figs. 1, 2).[14,15] We fabricated new bone graft materials in an attempt to meet all the requirements mentioned above by applying the RP technique to molding α-TCP powder.

Materials and methods

Fabrication of a tailor-made TCP implant

Computed tomography (CT) of the cephalic skull portions of seven beagles was performed under sedation, using full-body type CT equipment (Medical Systems/Hi speed CT/I, GE, Stanford, CA, USA) with the slice thickness being 1 mm under the conditions of 120 kV and 180 mA. The CT data were converted to CAD data and 3D images were reconstructed using the software Mimics (Materialise, Leuven, Belgium). On the 3D images, square bone defects (15 mm × 15 mm) were created bilaterally, the center of which was located at a point 25 mm anterior and 15 mm lateral to the external occipital protuberance (Fig. 3A). Then, TIs for the defects were designed using STL modification and editing software Magics (Materialise). With this software, we created a total of six cylindrical holes inside the implants: three holes of 2 mm in diameter in the cranio-caudal direction and three in the axial-abaxial direction (Fig. 2), in the hope that such conduit structures might facilitate vascular invasion and bone regeneration. Using these data, the final TI design was determined (Fig. 2).

Ink-jet printing is a layer manufacturing technology that fabricates three dimensional models from CAD data. The process consists of forming layers (0.1 mm thick) by using a printer-like device to distribute an adhesive to bond the surface of a powder into the desired shape (Fig. 1). Liquid binder is ejected from the ink-jet printer (Z406 3D color

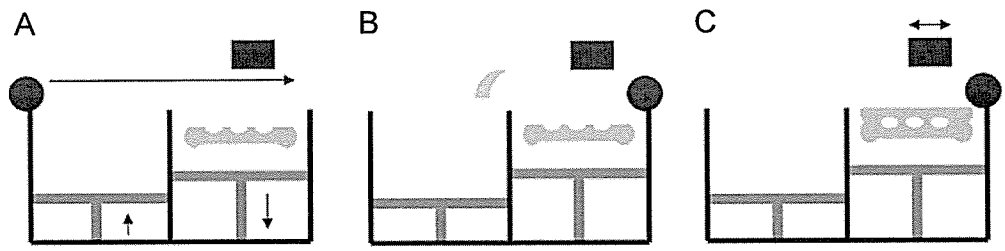

Fig. 1A–C. The ink-jet printing process. Ink-jet printing is a layer manufacturing technology that fabricates three-dimensional models from computer-aided design (CAD) data. The process consists of forming layers by using a printer-like device to distribute an adhesive to bond the surface of a powder into the desired shape. **A** A measured quantity of ceramic powder is first dispensed from a supply chamber on the *left* by the incremental upward movement of the piston. **B** A roller then distributes and compresses the powder at the top of the fabrication chamber on the *right*. **C** The jetting head subsequently deposits a liquid adhesive in a two-dimensional pattern onto the layer of powder, bonding the areas into the desired shape. These steps are repeated until the whole part is formed within the fabrication chamber

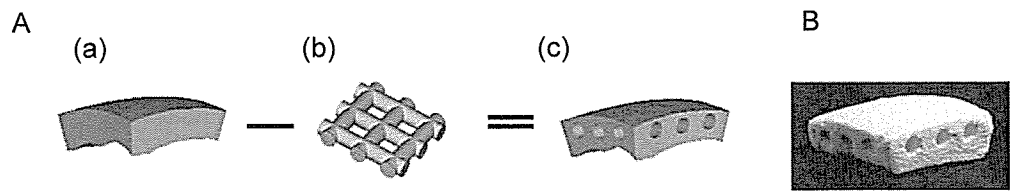

Fig. 2A, B. Tailor-made tricalcium phosphate (TCP) implant. **A** The CAD model design of the implants was performed based on the computed tomography (CT) data of the skulls of seven beagle dogs. We converted the CT data to CAD data, creating a 15 × 15-mm virtual implant model (*a*) of the defects. Six perpendicularly intersecting circular cylinders 2 mm in diameter (*b*) were also fabricated using CAD, and were virtually removed from the implant model to produce the final implant design (*c*). **B** The taylor-made bone implant (TI) model was fabricated by the ink-jet printer based on the CAD model design data

printer: Z-corporation, Burlington, MA, USA),[15] and with the repetition of the hardening of the powder material on the flat surface (hydration), a solid figure is formed. The powder used was α-TCP (Biopex, Mitsubishi Materials, Tokyo, Japan)[16] with the mean particle diameter being 10μm. The binder agent was a mixture of 5% sodium chondroitin sulfate (Seikagaku, Tokyo, Japan), 12% disodium succinate (Wako, Osaka, Japan) and 83% distilled water (Otsuka Pharmaceuticals, Tokyo, Japan). For 1ml of powder, 0.1ml of the binder agent was applied. Figure 2B shows the outer appearance of the TI. The manufacturing precision was ±0.1mm. The porosity of the TI was 61% with the mean diameter of the micropores being 10μm. As a control, hydroxyapatite implants (HI) were cut manually from sintered hydroxyapatite porous blocks (Apaceram Pentax, Tokyo, Japan). The HI possessed micropores (several micrometers in diameter) and macropores (several hundred micrometers in diameter), with a porosity of 55%. The bending strength was 9MPa and the compressive strength was 20MPa.

Surgical procedures

This study was conducted under the Guidelines of the Animal Care Committee of the Graduate School of Agricultural and Life Sciences, the University of Tokyo. Beagle dogs (9.3–14.8kg body weight, 1–2 years old) were purchased from Nosan Corporation (Kanagawa, Japan). No abnormalities were observed in the pre-experiment physical examination, blood test, or blood chemical analysis. Animals received midazolam hydrochloride (0.1mg/kg, im) and butorphanol tartrate (0.2mg/kg, im); then anesthesia was induced by intravenous propofol (3–6mg/kg) and maintained by inhalation of isoflurane and oxygen. After the routine preparation of the surgical field,[17] the cranial bone surface of the region was exposed. Measuring the length correctly with slide calipers on the basis of the external occipital protuberance, marks were placed for the location of the bone defect according to the preoperative planning on the 3D images. Two bone defects were created in the skull by a round bar and a sagittal saw (Stryker Instruments, MI, USA). After irrigation of the defect sites with sterile saline, a TI was implanted on the right-hand side and an HI

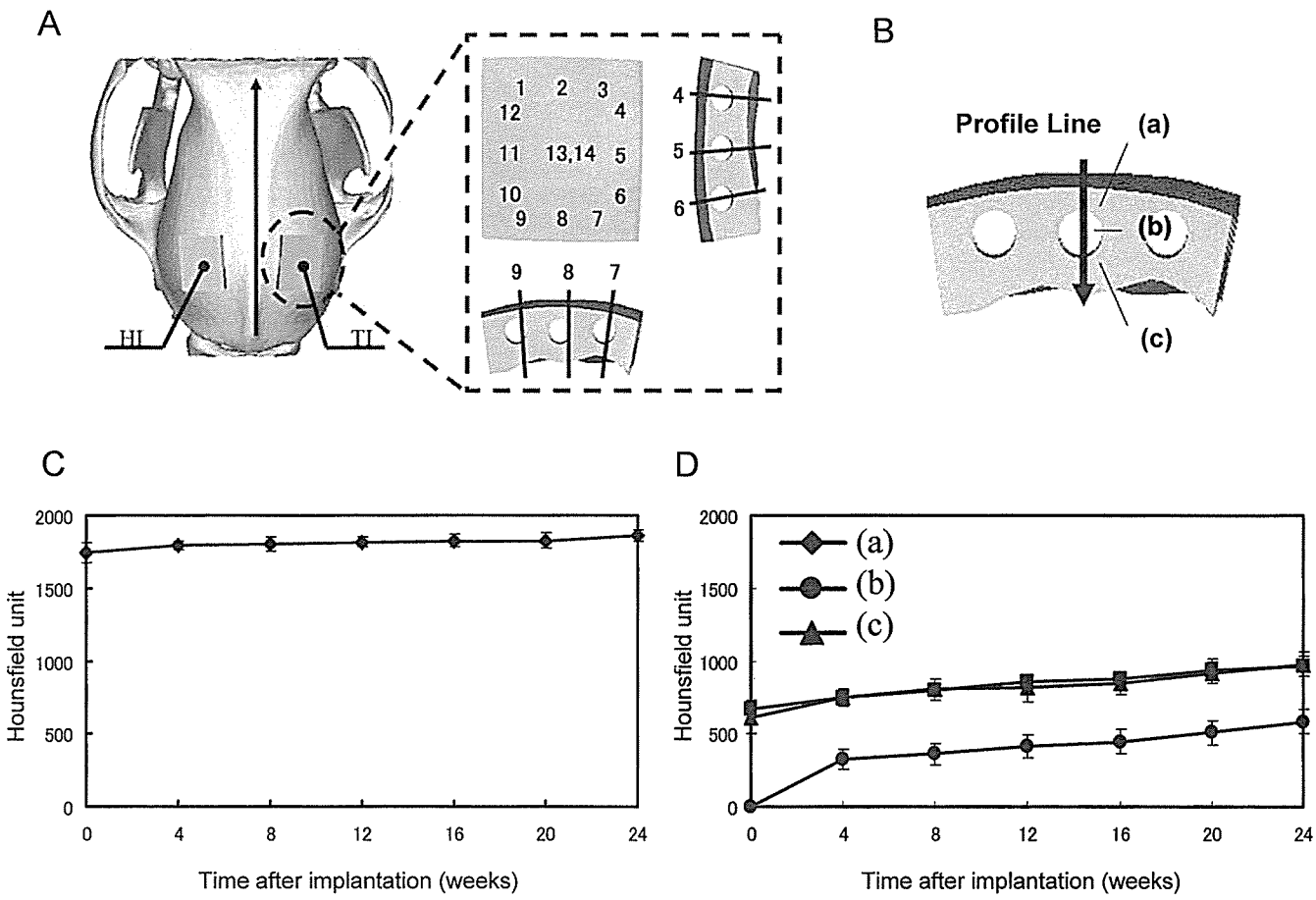

Fig. 3A–D. CT measurements. **A** Measurement points 1–14 were selected as shown. The measurement points 1–3, 7–9, and 13 were analyzed from the CT image of the slices perpendicular to the sagittal suture. The other measurement points were analyzed from the slices parallel to the sagittal suture. *HI*, hydroxyapatite implant. **B** For each point, the CT values of the subpoints above the cylindrical hole (*a*), through the center of the hole (*b*), and below the hole (*c*) were measured. **C** and **D** Changes in the mean CT values of subpoints *a*, b, and c. **C** The CT values of HI did not show any significant change for any subpoints; **D** however, the CT values of TI at all three subpoints increased